Universidade de Aveiro
2011

Departamento de Física

Telmo David Pelicano Almeida

Caracterização do Regime Transiente em EDFAs

EDFA transient regime chacterization

Universidade de Aveiro
2011

Departamento de Física

Telmo David Pelicano Almeida

Caracterização do Regime Transiente em EDFAs

EDFA transient Regime characterization

Dissertação apresentada à Universidade de Aveiro para cumprimento dos requisitos necessários à obtenção do grau de Mestre em Engenharia Física, realizada sob a orientação científica do Dr. Paulo Sérgio de Brito André, Professor Auxiliar Convidado do Departamento de Física da Universidade de Aveiro e Investigador Auxiliar do Instituto de Telecomunicações.

Dedico este trabalho aos meus pais pelo incansável apoio e educação que me deram.

O júri

Presidente	**Prof. Drª. João Filipe Calapez de Albuquerque Veloso** Professor Auxiliar, Departamento de Física da Universidade de Aveiro
Arguente	**Drª. Berta Maria Barbosa Neto** Investigadora, Nokia Siemens Networks
Orientador	**Prof. Doutor Paulo Sérgio de Brito André** Professor Auxiliar convidado, Departamento de Física da Universidade de Aveiro

agradecimentos

Considero que este trabalho é o culminar de um percurso académico de cinco anos, cujos sucessos se devem ao contributo e ajuda de muitas pessoas.
Primeiramente quero agradecer a todos os colegas de curso que me ajudaram e estudaram comigo, com um agradecimento especial aos colegas de estudo e de laboratório em várias cadeiras André Albuquerque, Bruno Faria, e Fábio Pereira. Sem as horas enumeras em que o Fábio e o André passaram a estudar comigo não teria tido tanto sucesso, e sem a ajuda e conselhos do Bruno as interfaces Gráficas deste trabalho teriam sido ainda mais difíceis de programar. Ao André também agradeço por me ter ensinado a aplicar o método de Runge-Kutta no Matlab, pois foi a chave para muitos dos meus problemas.
Quero também agradecer ao professor Fernão Abreu por me ter ensinado a abordar os problemas como um Engenheiro Físico e por ter sido o primeiro professor a acreditar e a apostar em mim.
Quero também prestar um grande agradecimento ao professor Paulo André, por todos os conhecimentos que me transmitiu pacientemente e todas as oportunidades que me deu para trabalhar como Investigador, estou profundamente grato.
Por toda a ajuda no laboratório no decorrer deste trabalho quero agradecer aos meus colegas do projecto GPON-in-a-box, em particular ao José Girão por me ter ensinado quase tudo o que sei hoje no que toca a trabalho laboratorial em redes ópticas. Não me posso esquecer também de toda a ajuda e lições que o João Prata me deu desde que cheguei ao IT.
Quero agradecer à Rita, que ao longo destes cinco anos foi a melhor companheira, a melhor das razões para lutar por um futuro promissor.
Por fim, quero agradecer a todas as entidades que me apoiaram e possibilitaram todo este magnífico percurso científico: Instituto de Telecomunicações(UA), Universidade de Aveiro(UA), Fundação para a Ciência e Tecnologia (FCT) e Agência para a Inovação (ADI).

palavras-chave EDFAs, transiente, interface gráfica.

resumo

O presente trabalho propõe-se a relatar o desenvolvimento de duas interfaces gráficas para a simulação dos modelos estacionário e dinâmico de um amplificador de fibra dopada com érbio (EDFA), bem como a caracterização experimental do regime transiente em EDFA's originado por tráfego em modo de rajada. Relata também a validação experimental bem sucedida do modelo dinâmico no que toca a simular os referidos perfis de tráfego.
É também descrita a avaliação experimental bem sucedida do impacto na geração de transientes de parâmetros importantes como o tamanho dos pacotes e o intervalo de tempo entre si, e a potência da bomba de um EDFA.

keywords EDFA, Transient, Graphical User Interface.

abstract

This work relates the development of two graphical user interfaces for the simulation of both the dynamic and steady state models of an erbium doped fiber amplifier (EDFA), as well as the experimental characterization of the transient regime of EDFAs when amplifying bursty traffic profiles. The experimental validation of the numeric model for simulating bursty traffic is also reported.

Experimental assessment of important parameters such as packet length, idle time duration and pump power was also performed and reported.

Index

1- Introduction

1.1 Motivation and state of the art

In the past decade, the impact and growth of Internet traffic cannot be left out from the spotlight. If at the beginning of the decade scientists and industrialists were expanding and adapting the concept of the Moore's law into the telecommunications industry, a few years later it was clear that the idea of an "Optical Moore's law" was going to be a misleading and meaningless concept by the year 2025, where even the most conservative models point out that the currently installed optical network would not be able to support the increasing demands for traffic [1-2]. An illustration of this exponential increase is presented in figure 1, where a projection of lit submarine-cable capacity growth is shown.

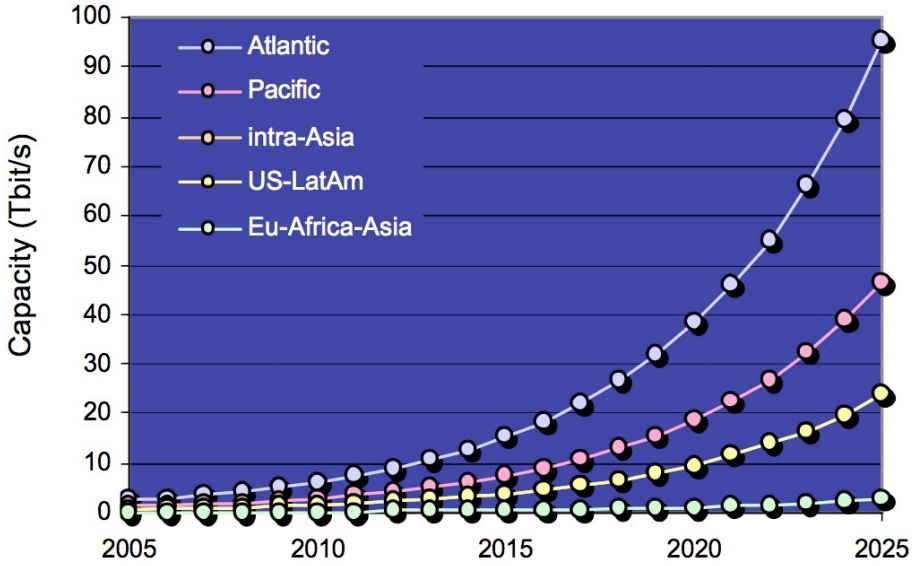

Figure 1: Projection of lit submarine-cable capacity until 2025 assuming a 20% yearly growth[2].

In telecommunications, fiber optic technology evolved from being the best solution for replacing copper cables in long haul transmission systems to be the core device for an entire platform capable of generating great value trough concepts like FTTH (fiber to the home) service providing [3]. Such feat is only possible throughout the employment of a set of technologies and devices that allow these networks to be transparent, fast, easy to monitor, and most importantly affordable to maintain and implement. Amongst these technologies and devices, wavelength division multiplexing (WDM) enhances the capability of optical fiber transmission systems by enabling many distinct wavelengths carrying different signal channels simultaneously, and the use of Erbium-doped fiber amplifiers (EDFA's) greatly improves the performance of these networks by overcoming the problem of attenuation and distortion of signals in long distance transmission systems [4].

Nowadays, innovations in WDM devices and modulation formats allow affordable scenarios at bitrates higher than 10 Gb/s with auto-reconfiguration capabilities, meaning that the network itself is able to switch, add and drop channels according to traffic demands [5].

Erbium doped fibers were first suggested as an amplifier for the third spectral telecommunications window by Payne et al in 1987 [6]. Since then they have been a part of every existing optical fiber project [7]. Nowadays, the typical span length between EDFAs in transmission systems is around 40–100 km [8] and the gain ranges from 40 to 50 dB [9], depending on several physical parameters that will be discussed in chapter 2.

Nevertheless, there are several issues related to the behavior of these amplifiers that have to be surpassed in order to obtain a more efficient output and consequently a better overall network performance. One of the main issues is the transient response of EDFA's when amplifying determined traffic profiles. For instance, in WDM networks, the signal level of each channel fluctuates due to channel add/drop or active rearrangement of the network [10]. Other example is bursty traffic, where data packets are assembled into bursts into their respective channel and transported across the optical network to the destination. The existence of long inter-burst idle intervals (from nanoseconds to seconds) enhances the transience nature of the EDFA response. Transient regime is cumulative as it propagates through multiple amplifiers, and thus its associated time constant becomes shorter, seriously jeopardizing packet integrity and consequently the overall objective of successful propagation of information throughout the network [11].

The interest in EDFA's over the past two decades as resulted in the creation of theoretical models to analyze both physical and performance aspects of the amplifiers [12]. Simulation software plays a key role at both research and commercial panoramas, because it allows cost saving performance optimization and in general it is a valuable tool when it comes to decision making before buying an expensive piece of equipment. However, most of the software solutions available in the market are either complex, costly, or both and therefore not accessible to every user [13].

Commercial software source codes are closed, preventing community development and deeper personalization that could boost important improvements. Developing open-source simulation software with familiar tools is a great asset because it covers all the features described in the last paragraph in a fresh perspective and also gives students a learning tool which was previously inexistent.

The aim of this thesis was to develop new open source software tools that could be useful in the laboratory and classrooms of the university and also experimentally perform relevant characterization of transient behavior in important traffic WDM scenarios.

1.2 Original Contributions

In an innovative approach, a Graphical User Interface (GUI) model was created for the study of EDFA general properties using a steady-state model.

Following the concept of creating GUIs, an interface was created in order to access with detail the add/drop impact in a network. The model itself is capable of doing calculations virtually for an infinite number of channels and operations.

The impact of bursty traffic was studied simultaneously in experimental and simulation environments.

This work produced three publications. The first is entitled “GUI model for simulation of steady state Erbium dopped fiber amplifiers” and was presented in poster form in the 2011 Eurocon and Conftele held in Lisbon.

The second one is entitled “Simplified Numerical Simulation of Bursty Packet Traffic Amplification by an Erbium-Doped Fiber Amplifier” was submitted to the 2011 IQEC/ CLEO Pacific Rim Conference that is to be held on the 28 of August 2011 in Sydney, Australia.

Finally an article entitled “Improved simulation method for QoS degradation due to bursty traffic in EDFAs” was submitted to Microwave and Optical Technology Letters.

1.3 Thesis Organization/Outline

This thesis is organized in the following way:

In chapter 1 the motivation and state of the art of are presented. Chapter 2 deals with the most relevant theoretical aspects of EDFA's and WDM networks. Chapter 3 presents the models that were developed along with several simulation results while chapter 4 explains all the experimental work followed by the correspondent interpretation of obtained data.

The last chapter draws final conclusions and analyses future perspectives and improvements that could be made both in the experimental and simulation panoramas.

Chapter 2- Theoretical background

2.1- Associated Phenomena

By definition an optical amplifier is a device that amplifies an optical signal without the need of optical-electrical conversion.

A fiber amplifier is an optical amplifier using an optical fiber as the gain media. In the case of doped fiber amplifiers optical fibers are doped with rare earth elements with different properties that will fundamentally lead to different amplification bandwidths and gain profiles.

Erbium is the most suitable dopant, since it allows amplification in the C band (1530nm-1565nm), which is the most used spectral region in current optical communications systems [14].

Stimulated emission is the phenomenon responsible for signal amplification in EDF's. To explain this concept stimulated absorption and spontaneous emission must be also referred, since they are complementary phenomena with relevance in the amplification process.

Considering a medium where atoms are characterized by two energy states: the fundamental state, with energy E_0 and the excited state with energy E_1 ($E_0<E_1$). In the presence of radiation with frequency ν a transition of some atoms to their excited state is observed:

$$\nu = \frac{E_1 - E_0}{h} \qquad (2.1)$$

being *h* the Planck constant. This process is designated by stimulated absorption.

Once in its excited state, an atom may emit a photon of frequency ν and return to its fundamental state. This process is called spontaneous emission because it occurs without external influence [15].

When a photon with the same frequency induces the process, the phenomenon is called stimulated emission. In this case, the emitted photon has the same characteristics than the stimulating photon (phase, polarization, direction and frequency).

A representative scheme of stimulated emission can be seen in figure 2.

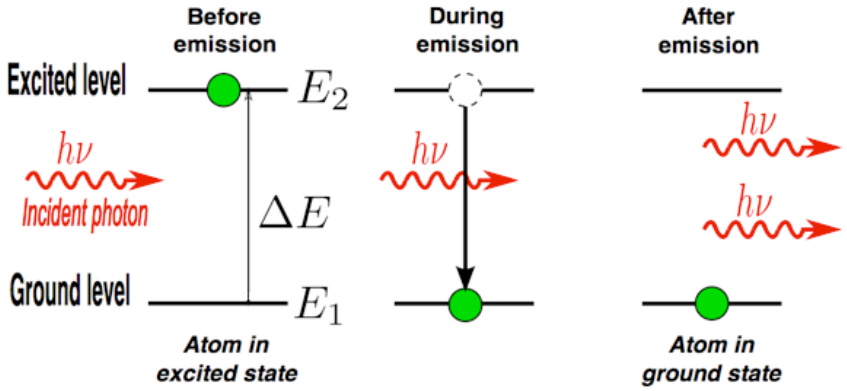

Figure 2: Representative scheme of stimulated emission [15].

Stimulated emission is a key phenomenon. It generates photons with the same characteristics as the incoming signal photons and thus signal amplification. However, spontaneous emission is a problem. This is due to the fact that the photons produced by spontaneous emission have random characteristics that generally differ from the signal and contribute as noise. This particular noise is known as ASE (Amplified Spontaneous Emission) and is one of the disturbing factors of the amplification process.

Rare earth elements are defined in the periodic table as the elements with atomic number Z between 57 and 71. Erbium, in particular, has the atomic number 68. In general, the atomic radius increases with the increment in atomic number but that is not the case for rare earth elements. In rare earth elements, levels 5s (n=4, l=0) and 5p (n=4, l=1) have 56 electrons. The remaining atoms are placed in the 4f level and are shielded by electrons of levels *5s* and *5p*. This shielding effect is responsible for the absorption and emission spectra of Er^{3+} that can be seen in figure 7 [16].

In the case of Erbium doped fibers, Er^{3+} ions are trapped in a glass host, originating a permanent electric field. As a consequence, an induced Stark effect splits the energy levels. These energy levels have their respective total angular orbital momentum, J that is split into a manifold of energy sublevels g= J + 1/2. A three-level Jablonski diagram shown in figure 3 can illustrate this phenomenon.

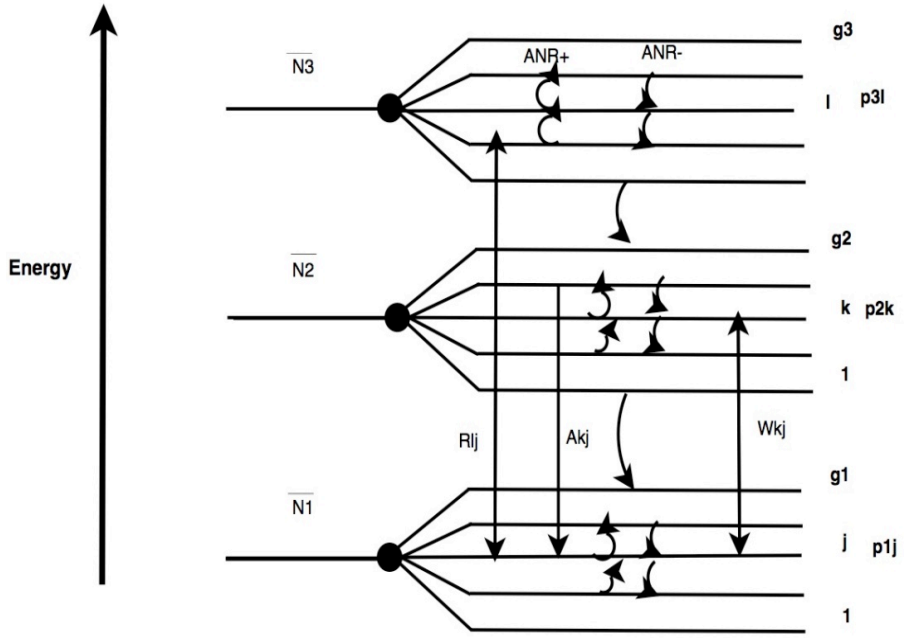

Figure 3: Energy level diagram corresponding to a Stark split three level laser system. The symbols $A\pm_{NR}$ indicate the thermalization between adjacent Stark sub-levels, while *W* and *A* denote stimulated and spontaneous emission or absorption rates, respectively and *R* pump rate [17].

However, population distribution between the manifolds remains constant due to thermalization (Boltzmann distribution), and it is valid to represent the lasing system with three single levels. This representation can be seen on figure 4 [17].

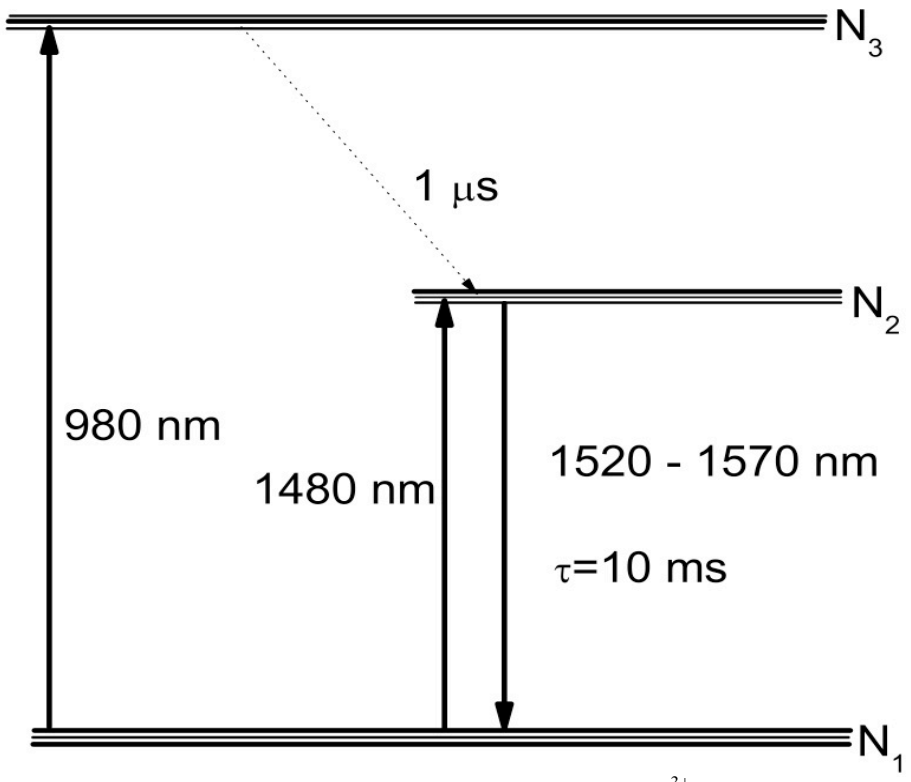

Figure 4: Generic three-level diagram for Er^{3+} [17].

In an EDFA, amplification occurs in four main stages. Firstly ions in the fundamental state N_1 are excited trough external pumping. Pumping effectiveness is the reason why Er^{3+} is generally depicted as a three-level system, because 980 nm and 1480 nm are the most effective pump wavelengths [18].

After pumping, ions are excited to a superior level of energy, N3 from where they quickly decay (1μs) to state N_2, which is the state where the amplification phenomenon described before will occur. The excited lifetime, τ, of state N_2 is about 10 ms, which is long enough for full population inversion and proper lasing conditions. Finally, photons from the transmitted signal induce stimulated emission and consequently light amplification [18].

An approach towards simplifying the theory behind EDFA dynamics was presented by Bononi et al in 1998 [19]. The EDFA is seen as a reservoir of excited state population that is depleted as signal photons come in.

The illustration of this concept is presented in figure 4.

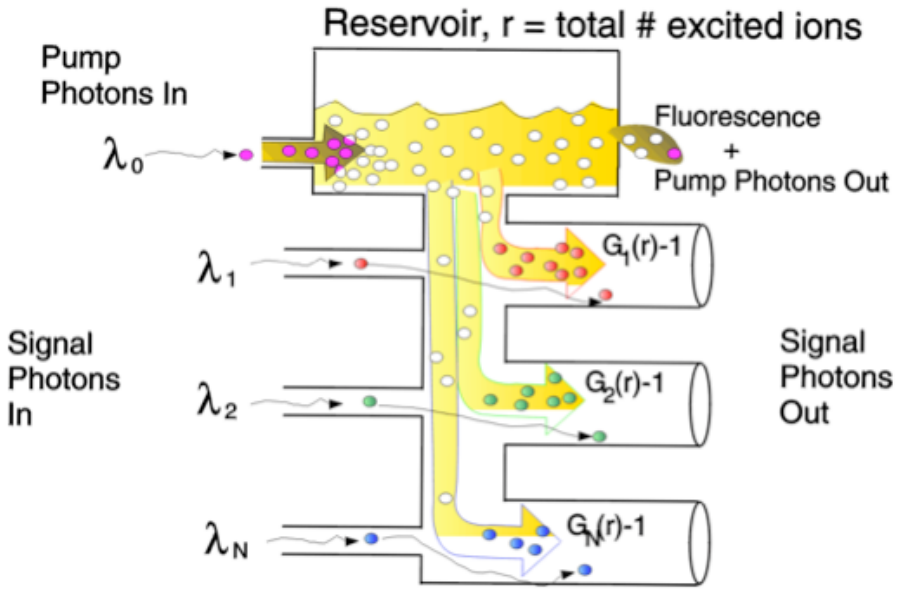

Figure 4: A simple, but correct way, of thinking about the amplification process in the EDFA [19].

The "reservoir approach" is also particularly useful to explain the basic nature of transients in EDFAs for both the bursty traffic and the add/drop cases. For the case of bursty traffic, packet distortion is due to the fact that the "reservoir" is full for the first incoming bits and that results in greater amplification than the following bits that are progressively affected by continued excited state population depletion.

An example of a packet affected by bursty traffic is presented at figure 5

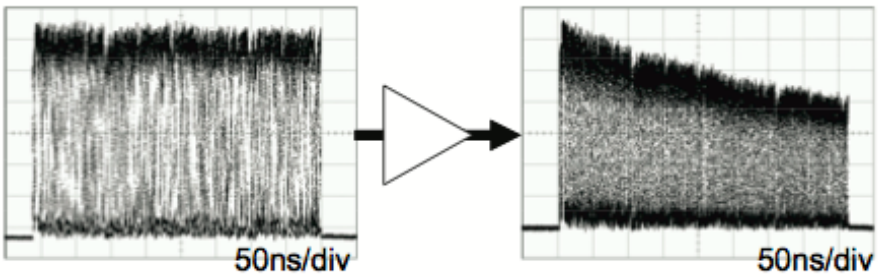

Figure 5: Packet affected by transient response of an amplifier [20].

For the power transients that arise due to the adding and dropping of channels, the explanations lies in the number of channels. If one or more channels are added, that represents a quick depletion in the reservoir and consequently a power transient. The same happens for dropping operations, where the power of the surviving channels quickly rises due to sudden rise in numbers of excited-state ions in the reservoir.

An image of a simulated 16 channel scenario that suffers an 8 channel drop is depicted in figure 6 and illustrates the quick rise in power of the surviving channels.

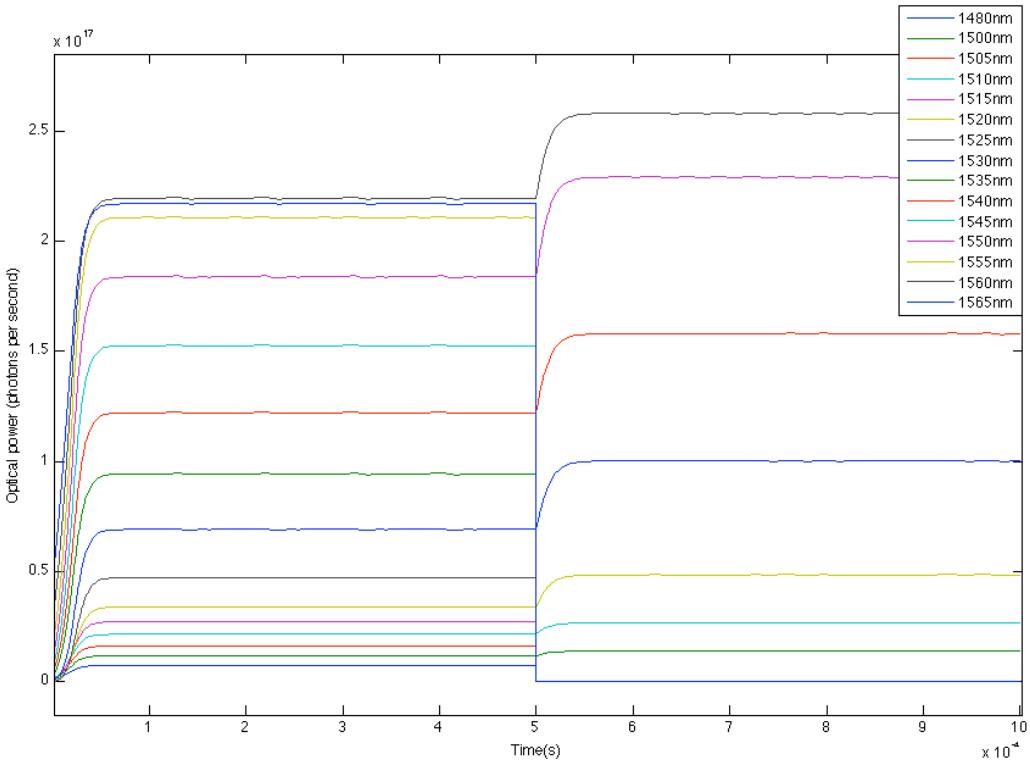

Figure 6: Simulated 16 channel scenario that drops eight channels at 0.5 ms

2.2- Intrinsic Parameters and Rate Equations

In this subchapter the important intrinsic parameters that are part of the simulation models are described.

When a signal with intensity I_s and a wavelength, λ_s, crosses a section of an EDF with infinitesimal thickness, *dz,* and atomic densities, N_1, and N_2, the intensity dI_s is given by:

$$dI_s = \{\sigma_{21}(\lambda_s)N_2 - \sigma_{12}(\lambda_s)N_1\}I_s dz \qquad (2.2)$$

where $\sigma_{12}(\lambda_s)$ and $\sigma_{21}(\lambda_s)$ are the absorption and emission cross sections of the laser transition at λ_s, respectively. The emission and absorption cross sections spectra for Er^{3+} doped alumino germanosilicate silica are displayed on figure 7. This typical values are used in all the modeling presented in chapter 3.

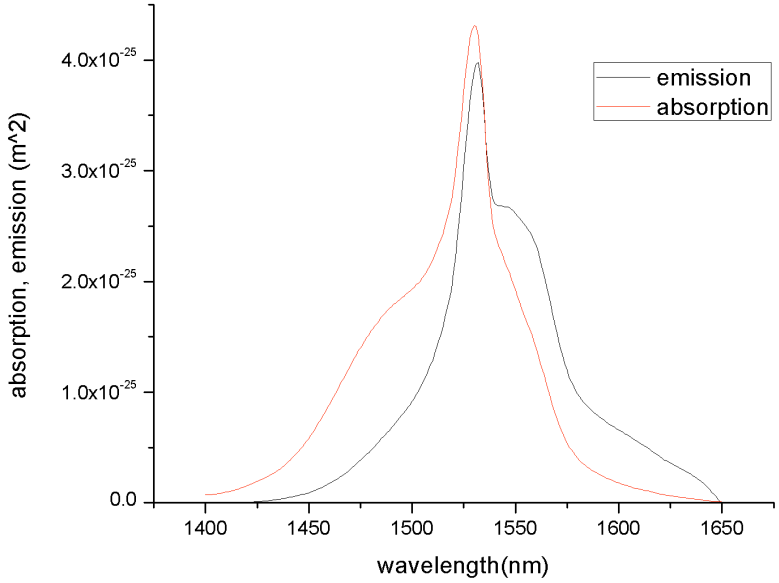

Figure 7: Emission and absorption cross sections spectra for alumino germanosilicate Er^{3+} glass fibers [17].

For the dynamic scenarios simulations the Giles parameters were also used. These were first introduced by Giles and Desurvire [21] and are the absorption coefficient α(λ) of the fiber with all laser-active ions in the ground state and the gain coefficient g*(λ) for the correspondent upper level ions.

These coefficients are dependent on the overlap factor, Γ(λ), between the optical modes and dopant density.

$$\alpha(\lambda) = \sigma_a(\lambda)\Gamma(\lambda)n_1 \tag{2.3}$$

$$g^*(\lambda) = \sigma_e(\lambda)\Gamma(\lambda)n_1 \tag{2.4}$$

The Giles parameters are easily obtained by measuring absorption and full population inversion gain. The use of these coefficients in modeling overcomes the fact that the overlap factor, Γ, and dopant density, ρ, are parameters not provided by manufacturers and are hard to experimentally determine.

The overlap Factor takes a value between 1 and 0 that represents the overlap between the optical mode and the erbium ion distribution. Only the portion of the optical mode, which overlaps with the Erbium, will contribute to stimulate absorption or emission.

The used rate equations in this thesis are based on the Saleh model [22]. These equations are also used by major commercial applications, such as Virtual Photonics®, VPItransmissionMaker® and OptiSystem® [23].

The basic formalism is a set of two equations that are fundamental, being regarded as the starting point for both steady-state and dynamic-state models developed in this thesis.

These rate equations are based in a two-level lasing system with an arbitrary number of channels (one corresponds to the pump) of wavelength λ_k and power $P_k(z, t)$, travelling in a direction u_k=-1, corresponding to a counter-propagating scheme, or u_k=1 for a co-propagating situation.

The amplifier is seen as a fiber with a given length, L, a dopant density ρ, within a volume of cross-sectional area, A.

The rate equation for the fractional population of the upper state $N_2(z, t)$ is

$$\frac{\partial N_2(z,t)}{\partial_z} = -\frac{N_2(z,t)}{\tau} - \frac{1}{\rho A}\sum_{j=1}^{N} u_j \frac{\partial P_j(z,t)}{\partial_z} \tag{2.5}$$

where $N_1(z,t)+ N_2(z,t)=1$. The change of power in the k_{th} beam is given by

$$\frac{\partial P_k(z,t)}{\partial_z} = \rho u_k \Gamma_k \left[\left(\sigma_k^e + \sigma_k^a\right)N_2(z,t) - \sigma_k^a\right]P_k(z,t) \tag{2.6}$$

These last two equations are manipulated in the models described in the next chapter. Such modifications will allow faster computation times or even the inclusion of phenomena such as ASE and background loss.

Chapter 3- EDFA models and Graphical user interface

Almost all developed theoretical models are based on the same basic rate equations shown in the previous chapter, but with different approximations, accordingly to the problem in question [18].

Generally, EDFA models can be divided into two categories, steady and dynamic state models. In steady state models, all the input powers are time independent, approximation methods such as average power analysis (APA) [19] and the exclusion of parameters such as amplified spontaneous emission (ASE) or background loss greatly simplify the modeling whereas in dynamic models the different channels involved suffer a plethora of phenomena that disturb the powers over time, requiring more complex numerical methods and accounting of all involved parameters [14].

As expected, steady state models do not often correspond to real scenarios, but they are still valuable for quick assessments regarding the influence of basic parameters, such as pump or signal powers and wavelength. Dynamic models are suited to amplifiers operating in WDM access networks, where signals are constantly re-routed or extinct due to add/drop operations or simply network failure, resulting in significant perturbations in the amplifier's gain. [20]

Regardless of the steady or dynamic nature of the model, it is always necessary to reach a compromise between computation complexity and versatility of the model when it comes to describe different kinds of scenarios.

As mentioned earlier, the aim of this work was to create simulation platforms that are easily accessible to every user. In order to do so, two models were produced in the form of Matlab® GUI (graphical user interface), one for steady-state amplifiers and other for the dynamic case.

3.1- Steady-State EDFA Model

In an attempt to make a fully featured steady-state graphical interface, the Hogkinson improved average power analysis method [19] was implemented. This method already accounts for ASE and still allows fast computation time.

In this model, the EDFA is considered to be a two-level amplifying system, and the dopant distribution profile along the fiber is assumed to be rectangular with radial symmetry. The evolution of power along the fiber is a function of distance and is expressed as:

$$\frac{dP_k^{\pm}(z)}{dz} = \pm\left(\left\{\left(\sigma_{21}^k + \sigma_{12}^k\right)N_2(z) - \sigma_{12}^k - N_t\right\}\Gamma_k - \alpha_k\right)P_k^{\pm}(z) \tag{3.1}$$

where k is the channel identifier, the ± symbol distinguishes between forward or backward propagation, σ_{21} and σ_{12} are the emission and absorption cross-sections, respectively. Γ is the overlap factor between the Erbium ions and the distributed optical signal propagate in the fiber, N_t represents the total population density, N_2 is the excited state population density, P the optical power and α is the term representing background loss. This model, accounts for ASE, the power evolution along the fiber is described by:

$$\frac{dP_k^{\pm}(z)}{dz} = \pm\left[\left(\Gamma_i\left\{\left(\sigma_{21}^i + \sigma_{12}^i\right)N_2(z) - \sigma_{12}^i N_t\right\} - \alpha_i\right)P_i^{\pm}(z) + 2\sigma_{21}^i N_2(z)\Gamma_i h\nu_i \Delta\nu\right] \tag{3.2}$$

where *h* is the Planck's constant, *i* denotes the channel identifier and P_i is the ASE power of the corresponding channel.

Applying the average power analysis technique, the Erbium doped fiber is divided into elemental sections with 2.5 cm in length. Each sections has a uniform distribution of N_2 was considered for $N_2(z)$. This way, small signal traveling-wave amplifier solutions are invoked for each section:

$$P_k^{\pm out} = P_k^{\pm in} G_k(z) \tag{3.3}$$

$$P_i^{\pm out} = 2h\nu_i \Delta\nu (G_i(z) - 1) \tag{3.4}$$

$$G_{ki}(z) = \exp\left[\left(\left\{(\sigma_{21}^{k,i} + \sigma_{12}^{k,i})N_2(z) - \sigma_{12}^{k,i} N_t\right\}\right)z.\Gamma_{k,i} - \alpha_{k,i}\right] \tag{3.5}$$

$$n_{sp} = \frac{N_2}{N_2\left(1 + \frac{\sigma_{12}^{k,i}}{\sigma_{21}^{k,i}}\right) - \frac{N_t \sigma_{12}^{k,i}}{\sigma_{21}^{k,i}} - \frac{\alpha_{k,i}}{\Gamma_{k,i}\sigma_{21}^{k,i}}} \tag{3.6}$$

$P_k^{\pm out}$ represents all the output powers produced by the input powers $P_k^{\pm in}$, while $P_i^{\pm out}$ represents the ASE output power. $G_{k,i}(z)$ is the power gain at the position z along the fiber and n_{sp} is the population inversion factor.

Considering that the distribution of power is uniform along the fiber, the averaging of the power associated with each channel is performed,

$$\langle P_k \rangle = P_k^{\pm in} \frac{(G_k - 1)}{\ln(G_k)} \tag{3.7}$$

and the ASE term is given by

$$\langle P_i \rangle = 2hv_i \Delta v n_{sp} \left\{ \frac{(G_i - 1)}{\ln(G_i)} - 1 \right\} \tag{3.8}$$

the expression for the excited state population density is

$$N_2 = \frac{N_t \left(\sum_{k=1}^{M} \frac{\langle P_k \rangle}{P_k^{sat}} + 2 \sum_{i=1}^{N} \frac{\langle P_i \rangle}{P_i^{sat}} \right)}{1 + \sum_{k=1}^{M} \frac{\langle P_k \rangle}{P_k^{sat}} \left(\frac{\sigma_{21}^{k,i}}{\sigma_{12}^{k,i}} + 1 \right) + 2 \sum_{i=1}^{N} \frac{\langle P_i \rangle}{P_i^{sat}} \left(\frac{\sigma_{21}^{i}}{\sigma_{12}^{i}} + 1 \right)} \tag{3.9}$$

Being the saturation power, P_k^{sat}, is equal to

$$P_{k,i}^{sat} = \frac{hv_{k,i} \pi a^2}{\tau_{21} \Gamma_{k,i} \sigma_{12}^{k,i}} \tag{3.10}$$

Replacing the term N_2 in the gain expression, an expression for the gain of a single elemental section of fiber is obtained:

$$G_k = \exp \left\{ \left(\frac{-N_t \Gamma_k \left(1 + P_b - \frac{\sigma_{21}^k}{\sigma_{12}^k} P_a \right)}{1 + P_a + P_b} - \alpha_k \right) L \right\} \tag{3.11}$$

P_a and P_b are dummy variables, iteratively adjusted until the gain equation gives self-consistent results

$$P_a = \sum_{k=1}^{M} \frac{P_k^{in}\left(G_k - 1\right)}{P_k^{sat} \ln(G_k)} + 2\sum_{i=1}^{N} \frac{2hv_i \Delta v n_{sp}}{P_i^{sat}} \left(\frac{(G_i - 1)}{\ln(G_i)} - 1 \right) \tag{3.12}$$

$$P_b = \sum_{k=1}^{M} \frac{\sigma_{21}^k}{\sigma_{12}^k} \frac{P_k^{in}\left(G_k - 1\right)}{P_k^{sat} \ln(G_k)} + 2\sum_{i=1}^{N} \frac{\sigma_{21}^i}{\sigma_{12}^i} \frac{2hv_i \Delta v n_{sp}}{P_i^{sat}} \left(\frac{(G_i - 1)}{\ln(G_i)} - 1 \right) \tag{3.13}$$

This approximation allows computation times of about 30 s with a computer with 2Gb ram and 2.6Ghz dual core processor, a key aspect that is fundamental when building a GUI. As mentioned earlier, steady-state models are useful when we intend to study the influence of each individual parameter in the overall performance of the amplifier. Therefore it is important for the user to run quick routines and at the same time visualize all the values of the involved parameters, being able to edit them on the run and simultaneously access the immediate impact on the simulation. In order to provide such solution in a user-friendly-environment, a steady-state GUI that enabled the features described above was created.

As it can be seen in figure 8, the GUI consists of a single window. All the editable parameters are editable and shown in the right, close to the plot with the desired results.

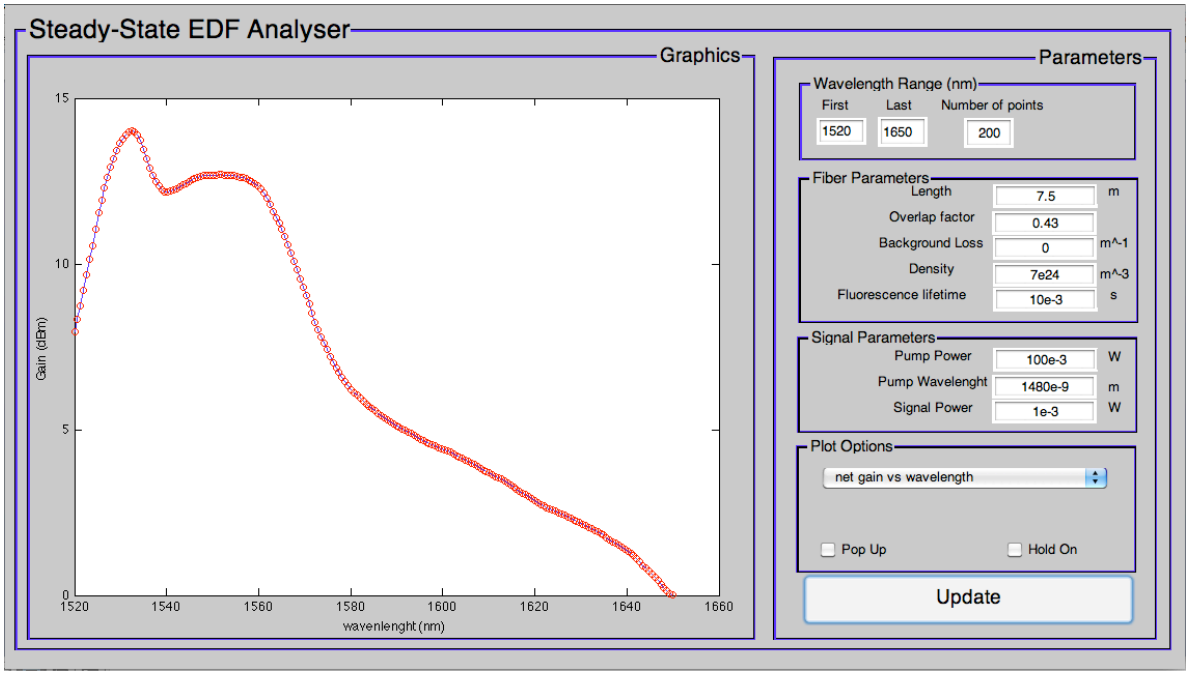

Figure 8: The developed steady-state Matlab GUI.

There is a number of plot options from which the user can choose. There is also the option to hold on the current plot so different results can be compared in the same window, or pop-up the current graphic onto a new window. In order to refresh the graphic, the user has to edit the desired parameters and press the "update" button. If neither the "pop up" or "hold on" boxes have a tick the GUI will simply replace the old plot with the new one. The plot options are located in the right bottom corner of the window, shown in detail in figure 9.

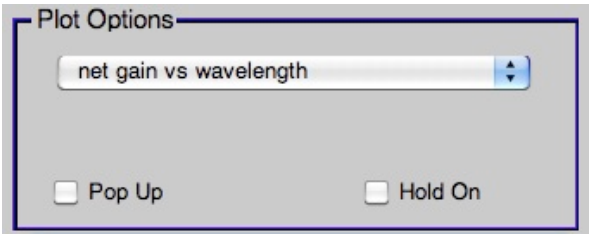

Figure 9: The GUI plot options area.

A rollover menu with several plot types is presented at this area. There are several plot types available, but since the GUI is completely open source and has all the constants and variables loaded in, users just have to edit three lines of the source code which includes help comments, and add a new plot option. This feature highly contributes to the versatility of this software. The current version of the GUI as several plot types built in and they can be seen in figure 10.

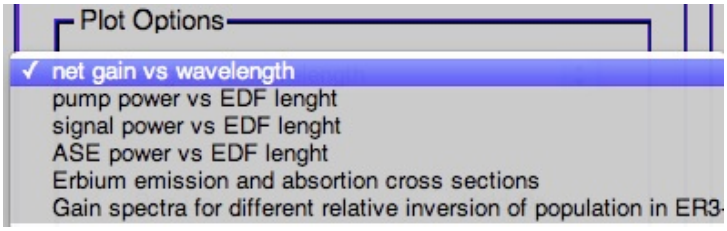

Figure 10: Roll over menu showing several plot types.

The parameter section was design to be a user friendly, simple to use control box. The editable parameters are disposed in three categories separated by frames. In the upper right corner we can see the wavelength range frame. Here the user is asked to input the first and last values for the spectral range and how many channels he wants to analyze within that range. The routine will create a linear space with the number of points the users specifies in the desired spectral range, being the maximum range [1400 1650].

Located below the wavelength parameters frame is the frame designated for setting the physical parameters of the fiber: Length, overlap factor, background loss parameter, density of doping and excited state lifetime. The unit of each parameter is indicated right next to each edit box. At last the signal and pump parameters frame where the pump and signal powers and wavelengths can be defined. This section and its respective frame can bee seen in greater detail in figure 11.

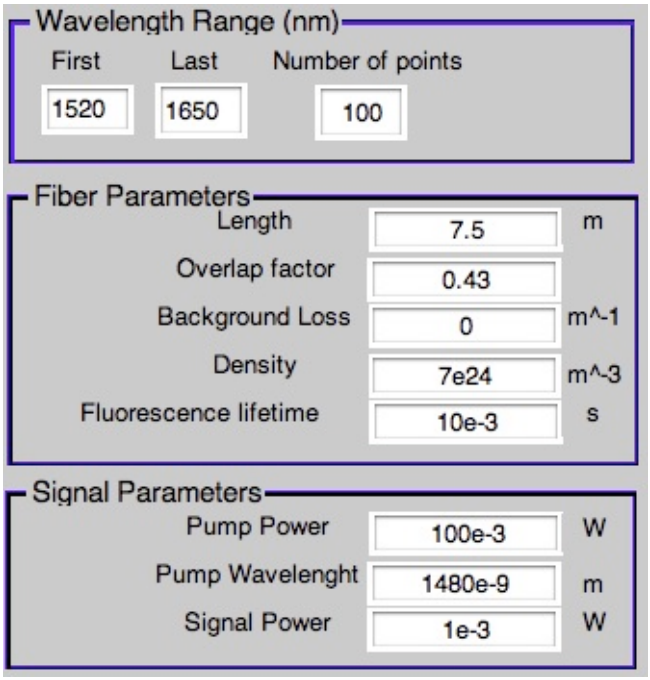

Figure 11: All the editable parameters.

The remaining element of the GUI is the graphics frame. It is the largest individual area of the GUI, occupying approximately half of the window. All the labels of the plots change automatically accordingly to the chosen plot type. Autoscale of the axes occurs every time the update button is pressed.

This current configuration is not at all mandatory. If the user has other needs or simply wants to give another aspect to the window, he can directly access the Guide tool in Matlab® and through simple clicking of boxes and "drag and drop" operations reshape the visual aspect of the GUI.

The simulator performance was tested for several working situations. In an EDFA, for a given length, the gain increases linearly with the pump power until a limit value, where the saturation occurs. As the pump power increases, more Erbium ions are excited producing more stimulated emission and consequently more gain. When all ions are excited along the fiber, the lowest energy level population of Erbium ions is fully depleted and increasing the pump power does not sort any effect, resulting in constant gain. This response was reproduced by our model and is illustrated in figure 12. A single signal channel at 1550 nm was used, the considered population density was 2×10^{24} m^{-3}, for an excited lifetime of 10 ms, an input power of 1 mW, a fiber length 10 m with a 1480nm pump varying power. The background loss was considered to be null.

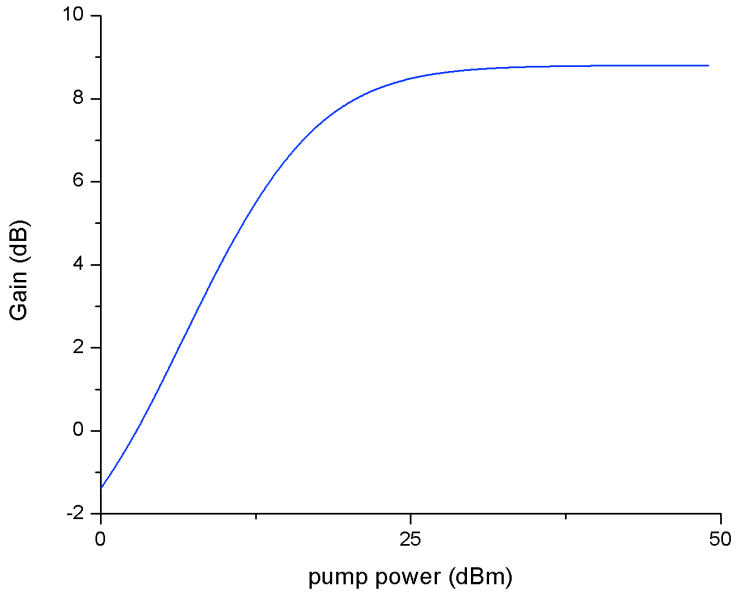

Figure 12: Gain as a function of the pump power.

A brief study regarding the influence of pump power value on the gain spectrum of the EDFA was also performed. The conditions were the same described above, with a 20 channel range between 1520 nm and 1560 nm. The chosen pump powers were 0 dBm, 10 dBm, 20 dBm and 30 dBm. It can be noticed that the gain does not tend to improve significantly once the saturation value is surpassed, even though the increment in power is always of one order of magnitude.

The results are presented in figure 13.

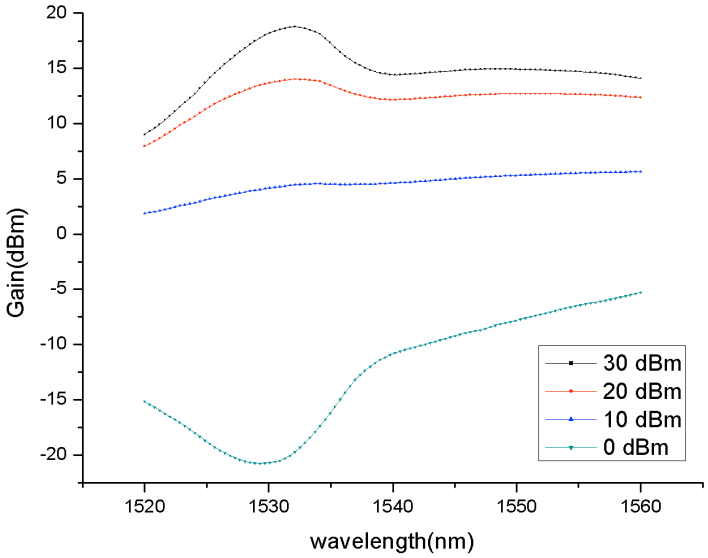

Figure 13: Gain profile in the 1520 nm-1560 1nm range for four different pump powers.

In an EDFA, the doped fiber length is an essential parameter, for long lengths, at the final end of the absorption of the signal that was amplified at the beginning of the fiber can occur. A long length allied with low pump powers can originate loss instead of gain while high powers and small lengths lead to an inefficient use of the available power budget. It can be affirmed that there is a strong correlation between fiber length, pump power and input signal power, and that for every fiber and purpose there is an optimum set of these values.

As a last example, we studied the impact of two different parameters: length and input power in the gain performance of the EDFA. Four fibers lengths were compared in this study. The lengths were 25 m, 50 m, 75 m and 100 m. A single channel was used, 1550 nm and the pump power was fixed at 20 dBm. The results can be seen in figure 14.

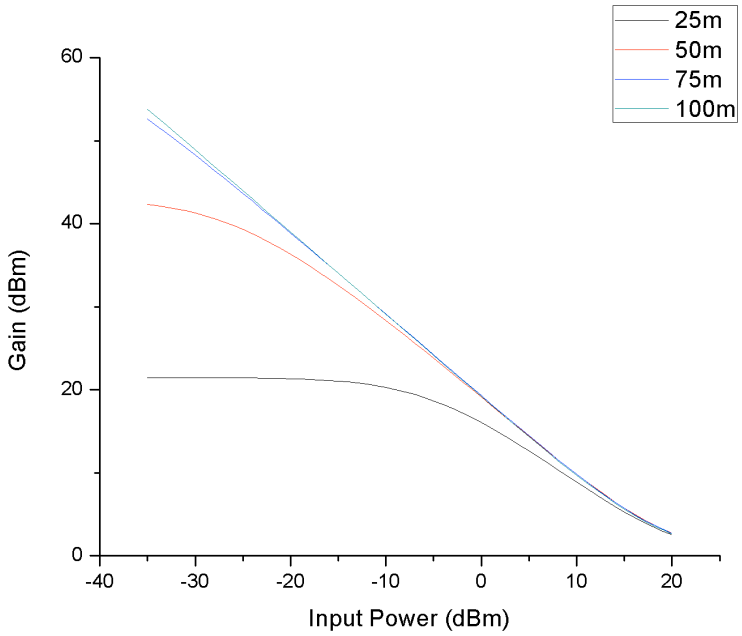

Figure 14: Input power as a function the gain for different fiber lengths.

The fixed pump power will supply a limited number of excited erbium ions and consequently a limitation to the amplifiers gain. For reduced input power the EDFA has enough upper level population for producing stimulated emission on all incoming photons but as the number of photons increases the EDFA is incapable of providing gain, quickly dropping in performance.

In an innovative approach, a steadty-state EDFA model was implemented in a GUI, using Matlab®. The result was an open-source software tool with quick computation times and easiness of use, especially when accessing the influence of a chosen parameter in the amplifiers performance, as the results can be quickly compared on the go, in the same window.

This implementation has a wide range of users, as it can be used for educational purposes, quick assessments before experiments or even as help for undecided buyers of EDFA's and EDF's.

Even with such great versatility, the open source format that uses simple tools like Matlab®'s guide function gives users a chance to customize and improve their experience with the software.

3.2- EDFA Dynamic Model

EDFA dynamic models are vital when it comes to simulate real network scenarios. In this work the purpose was to use them as a tool to study the transient behavior of the EDFAs response to add/drop operations or in presence of bursty traffic.

The simulation of such scenarios is vital to access the contribution of several different intrinsic parameters of EDFAs in the overall network performance. This is especially relevant in a dynamic reconfiguration network to guaranty that the most fruitful optimization is made.

For the characterization of both the add/drop problem and the bursty traffic problem a model proposed by Rieznik and Fragnito [23], based on the Saleh model (presented in chapter 2), was implemented. The Saleh model has a known analytical solution for its longitudinal dependence. However, the contributions of ASE and background loss are neglected.

By showing that the time dependent gain has an analytical solution if the excited state population is constant along the fiber, Rieznik and Fragnito proposed a more complete model, which already accounts for these two missing parameters.

The two equations of the Saleh model with the ASE and background loss terms included are the following:

$$\frac{\partial N_2(z,t)}{\partial t} = \frac{\partial N_2(z,t)}{\tau_0} - \frac{1}{\rho S}\sum_{n=1}^{M}\left[(\gamma_n + \alpha_n)N_2(z,t) - \alpha_n\right]P_n(z,t) \tag{3.14}$$

$$\frac{\partial P_n(z,t)}{\partial t} = u_n\left\{\left[\gamma_n + \alpha_n)N_2(z,t) - \alpha_n - \alpha_{loss}\right]P_n(z,t) + 2\gamma_n\Delta v(z,t)\right\} \tag{3.15}$$

Since all the simulations of this work deal with small fiber lengths and low power signals (<10 mW), background loss is negligible. Assuming that N_2 is constant along the fiber and integrating from 0 to L, the solution for equation 3.15 is

$$P_n^{out}(t) = P_n^{in}(t)G_n(t) + 2n_n^{sp}\left[G_n(t) - 1\right]\Delta v \tag{3.16}$$

with

$$G_n(t) = \exp\left\{\left[\left(\gamma_n + \alpha_n\right)N_2(t) - \alpha_n\right]L\right\} \tag{3.17}$$

$$n_n^{sp} = \frac{N_2(t)\gamma_n}{(\gamma_n + \alpha_n)N_2(t) - \alpha_n} \tag{3.18}$$

the solution for equation 14 is

$$\frac{dN_2(t)}{dt} = \frac{dN_2(t)}{\tau_0} - \frac{1}{\rho SL}\sum_{n=1}^{M}\left[P_n^{out}(t) - P_n^{in}(t) - 2\gamma_n \Delta v N_2(t) L\right] \tag{3.19}$$

This last differential equation is solved using the Runge-Kutta method and the equations 3.16, 3.17 and 3.18 are solved for a designated period of time.

For simulating add/drop scenarios, input power changes are introduced in the simulation as desired.

Computation times of approximately 1.9 s in a computer with 2GB RAM and a 2.66GHz dual core processor are that fast because the Runge-Kutta method is applied only when an add/drop operation occurs. An add/drop operation is by definition given for multiple adds, drops, or both in occurring at a given time. For instance, in a 32 channel scenario, a simulation is done for 1 s. At 250 ms, 500 ms and 750 ms, two chosen channels are dropped. This means that the simulation will solve four differential equations to determine the evolution of N_2 during the time periods of 0 ms -250 ms, 250 ms – 500 ms, 500 ms-750 ms, 750 ms-1000 ms.

In a computer with average specs, an equation takes approximately 1.9 seconds to be solved. These fast computation times allow a graphical user interface to be implemented and to serve the purpose of its predecessor but for the dynamic case. However, the dynamic nature of the problem poses a programming challenge. Firstly, the algorithm must be written in order to solve as many equations as it is required to do, accordingly to the users needs, and secondly, a proper interface needs to be designed, meaning that it has to transform itself to the users needs. If the user only wants to work with 2 channels, he should only input data for two channels, if he only wants one operation, he shall only have to input data for that given operation. The first problem was diced out by employing a set of two “for” loops and an operation matrix of ones and zeros, representing adds and drops. Each line of the operation matrix represents the state of each channel at that given time: if there is a one it means that the channel is added, if there is a zero, the channel is dropped. A loop that loads all the channels and calculates the Gain, spontaneous emission factor and output power is in its turn inside of a loop that multiplies the input powers by the lines of the operation matrix and solves the equation for the respective operation.

The only problem left relates to the design of the graphical user interface itself and the limitations of Matalb’s Guide Tool. Ideally, the user would define how many channels to simulate and how many operations to perform. This would mean that a separate window would have to be created and dynamically generate the boxes to input all the data. Besides all the complexity involved in coding and linking data between the two windows, the computation time would drastically be increased as the hardware processed the loading of all

the graphical elements. Also Matlab's Guide tool tends to drastically reduce its speed when many graphical elements (boxes, menus, axes, etc.) are being programmed. Despite all setbacks, a creative compromise was reached and an interface was developed, mostly for showcase purposes, so further improvements could be made in a near future, possibly in a more suitable programming language.

The maximum number of channels was limited to 8 and the maximum number of operations was limited to 4. The computation time issue was surpassed by loading the interface with all the edit boxes, corresponding to all the eight channels and four operations. Then if the user chooses a lesser number of channels or operations, the edit boxes of the unnecessary channels and operations disappear.

Figure 15 shows a picture of the main and only window of the interface.

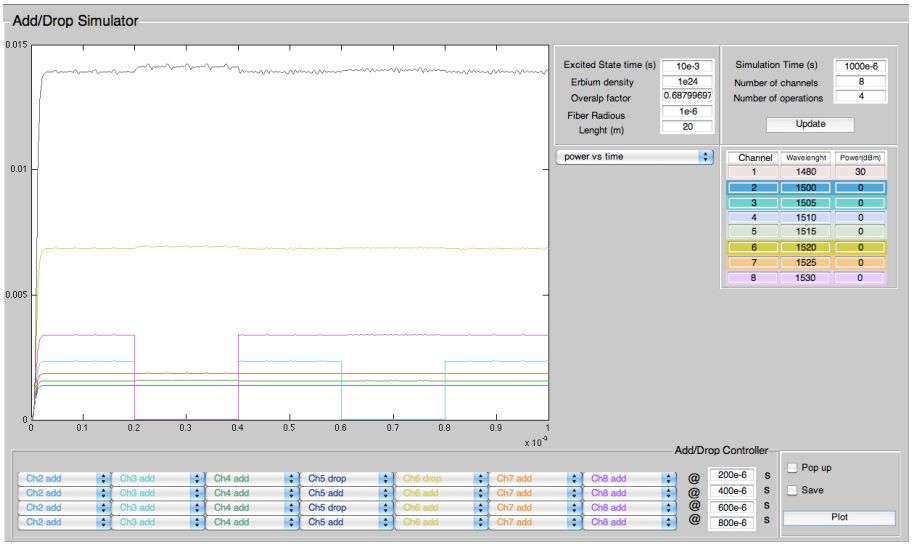

Figure 15: The developed dynamic Matlab GUI.

The interface allows the study of several add/drop scenarios and combinations. As its predecessor (the steady-state GUI), an area dedicated to the editing of the intrinsic parameters is present. It can be seen in greater detail in figure 16.

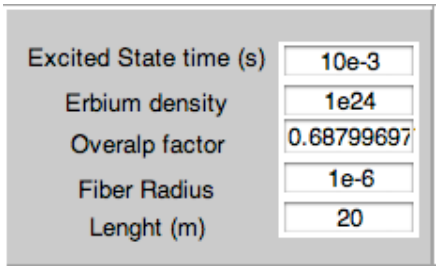

Figure 16: Intrinsic parameter edit box.

In a frame right next to the editable parameters the user defines the simulation time and the number of channels and operations to perform. These last two parameters will generate the necessary number of edit boxes and add/drop menus. The default case for 8 channels and 4 operations is shown in figure 17.

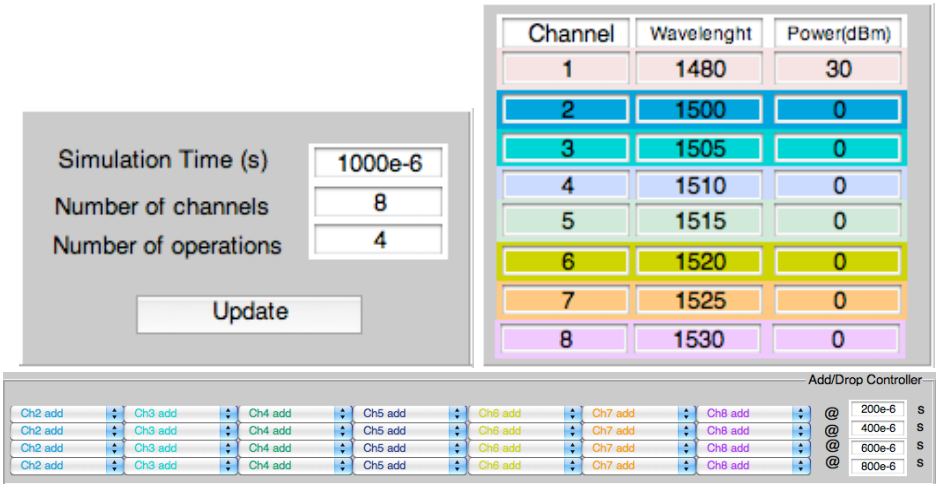

Figure 17: Configuration of the GUI with 8 channels and 4 operations.

As it can be seen, there is a frame where the channel parameters are inserted and an Add/Drop controller frame composed mainly of pop up menus, where the user defines if a channel is going to be dropped or added and when it will occur, up to four operations, by default every channel is added

This configuration is intuitive and fast, allowing the user to quickly add and drop channels and immediately access the impact of the changes. This principle is also valid for all the other parameters that are editable in the GUI.

As its steady-state counterpart, the dynamic GUI as also different plot options, in this case the user can choose if wants to analyze the evolution in time of the gain, spontaneous emission amplification factor or, more importantly and set by default, the power evolution along time. The pop up option is also present along with the possibility of saving currently plotted data in ASCII format so it can be used in other formats. A zoom function was also added so the user can study in greater detail the simulated scenarios.

One interesting exercise to do with the add/drop model is to compare the impact off pump power in the transient generation phenomenon because it is a parameter that can be easily controlled and optimized for minimizing the impact of adds and drops in the networks performance.

In figure 18 two graphics representing the same scenarios with different pump powers can be seen side by side.

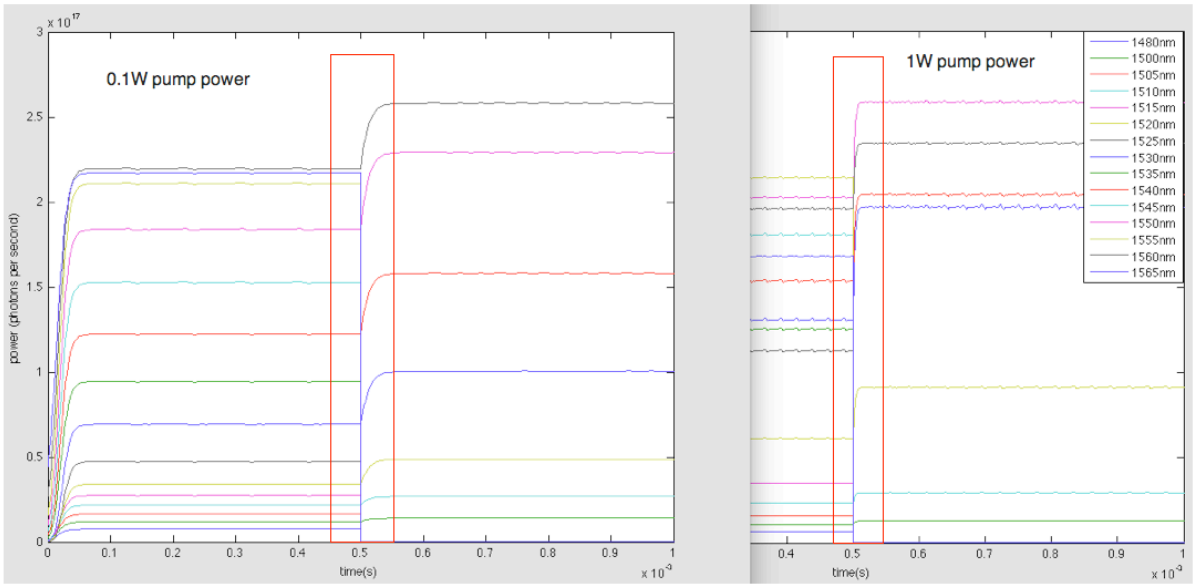

Figure 18: Scenario depicting 16 channels and at 500ms half the channels are dropped for two different pump powers.

It is clear that in this testing scenario, higher pump power represents less transient time due to saturation. A dynamic network with EDFAs operating in their saturation regime will suffer much more sudden changes and will not be able to re-configure itself as faster and effective as a network operating in non-saturation regimes. This shows that pump control is one of the most important parameters.

A final and vital aspect of the simulation work presented in this thesis is for bursty traffic simulation.

The numerical modeling of bursty traffic is implemented in a similar fashion of the add/drop model, which involves solving the same equation with the Runge-Kutta method, with the difference that it is solved for every single bit of a generated packet, bit by bit, using the last bit solution as an initial parameter for the next equation. This obviously implies a great computational effort, since pseudo random bit sequences (PRBS) up to 2^{15}-1 bits are generated, implying the resolution of 2^{15}-1 sequences.

The creation of a GUI for these types of simulations is pointless since calculations for one single packet takes 15 minutes in a good computer and even longer in average computers.

However, simulation of bursty traffic in such a simplified model can potentially be used in the designing of EDFAs optimized for the minimization of the transients due to the bursty traffic. Also, bursty traffic scenarios are easier to replicate in a laboratorial scenario where a few key components are needed, unlike add/drop scenarios where a large number of lasers and optical add/drop multiplexers (OADMs) are necessary. Bursty traffic is the basis of all the experiments that were carried out in the course of this work and is described in chapter 4.

An example of a bursty packet simulation is presented in figure 19. An initial sequence of zeros with idle time of 300 µs is first loaded, being the pump signal active. This is done in order to the amplifier achieve full population inversion before packet amplification starts. In this particular case, after the initial sequence of 300 µs with no signal, two 2^{15}-1 PRBS sequences with duration of 26 µs are separated by a defined idle time.

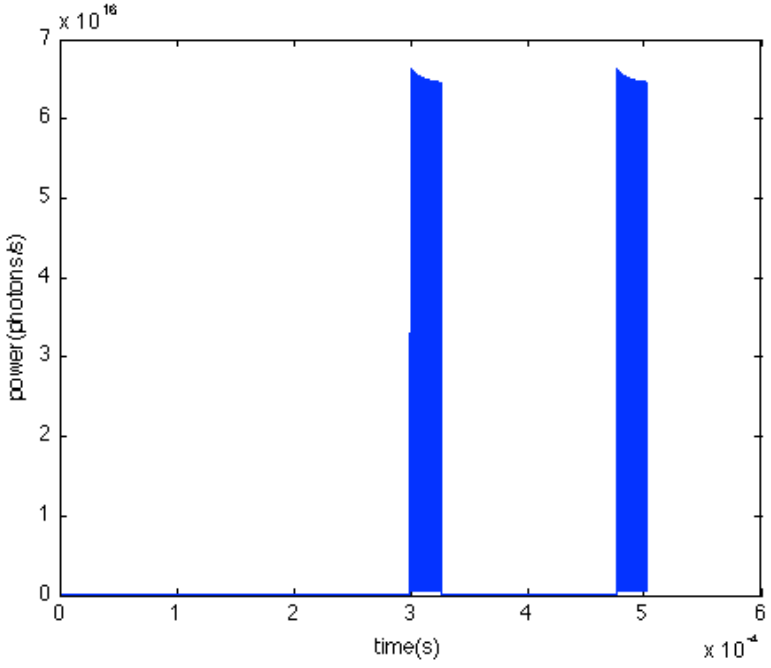

Figure 19: Simulated signal power amplified by a typical satured EDFA for two packets separated by an idle time of 150 µs.

Bursty traffic experimental work requires less equipment than an add/drop scenario. This allowed the design of an experience to validate the proposed computational model. The experiment and results are presented in the next chapter.

Chapter 4- Experimental Assessment

As mentioned briefly in the previous chapter, all the experimental work was focused on transient generation due to the presence of bursty traffic.

In order assess the impact of transience response of EDFAs in bursty traffic packets several experiments were carried on.

The experimental setup consists of an external cavity laser peaking at 1550.92 nm with an optical power of 13 dBm, followed by a polarization controller and a Mach-Zehnder optical modulator operating at 1.25 Gb/s. After the Mach-Zehnder the optical signal is amplified by an EDFA (IPG-500-C3-W from IPG Photonics), attenuated and received by a PIN photodiode (HP-11982A), being finally analyzed by an Agilent Infinium 86100A oscilloscope.

Customize packets were prepared, PRBS sequences of a defined number of bits followed by a sequence of zeros that would represent an idle time.

A schematic of the bits sequence used is shown in figure 20 and the experimental iplementation setup diagram is shown in figure 21.

Figure 20: Bits sequence used in experiments.

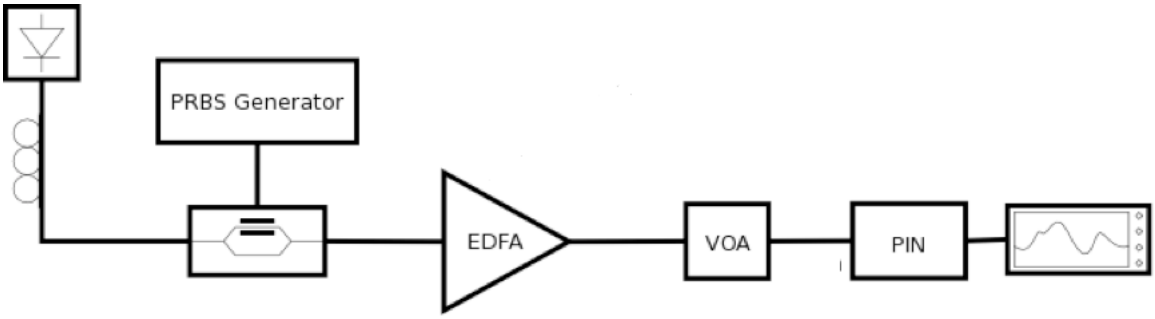

Figure 21: Implemented experimental setup.

The first experimental procedure relates to calibration, where the goal was to maximize the extinction ratio by adjusting the polarization controller and the Mach-Zhender drive voltage. The back-to-back signal and all electrical measurements are also done in order to assure that the system is generating data packets correctly. A typical eye diagram and the aspect of a correctly generated data packet are presented in figures 22 and 23 respectively. A PRBS sequence with several packets can be seen in figure 24.

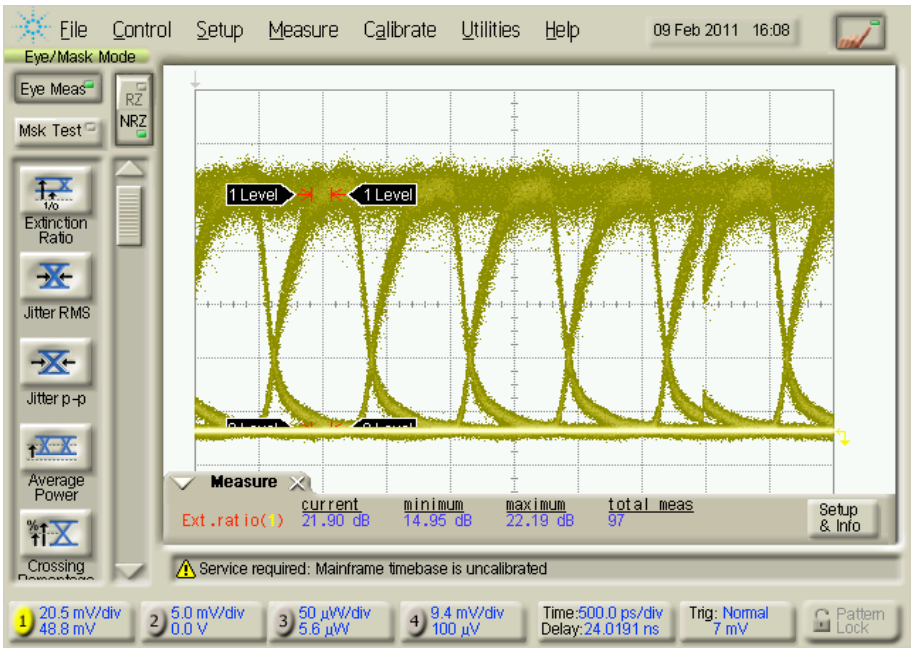

Figure 22: Experimental signal eye diagram.

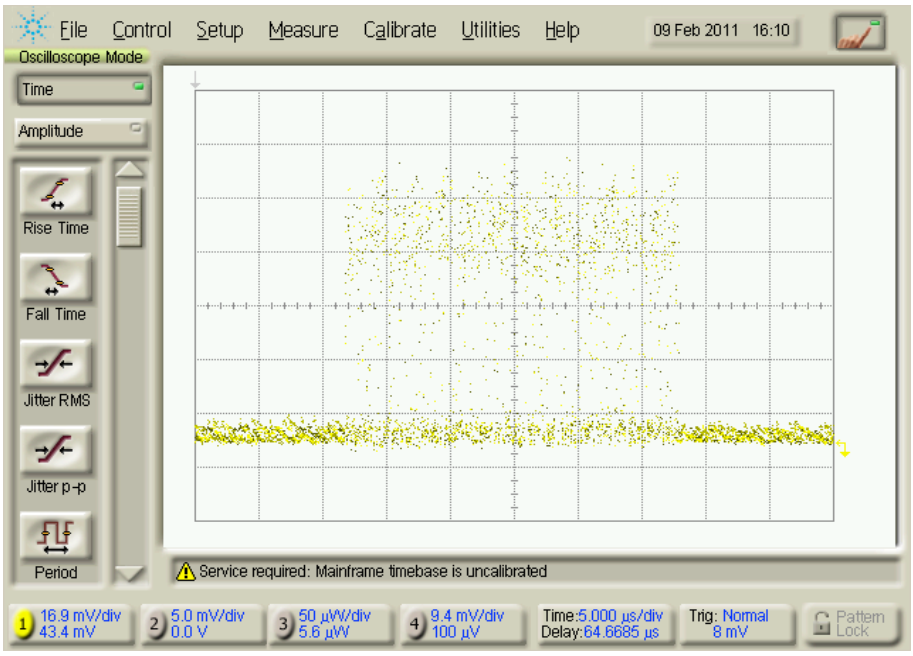

Figure 23: Back-to-back signal for a PRBS 2^{15}-1 data packet.

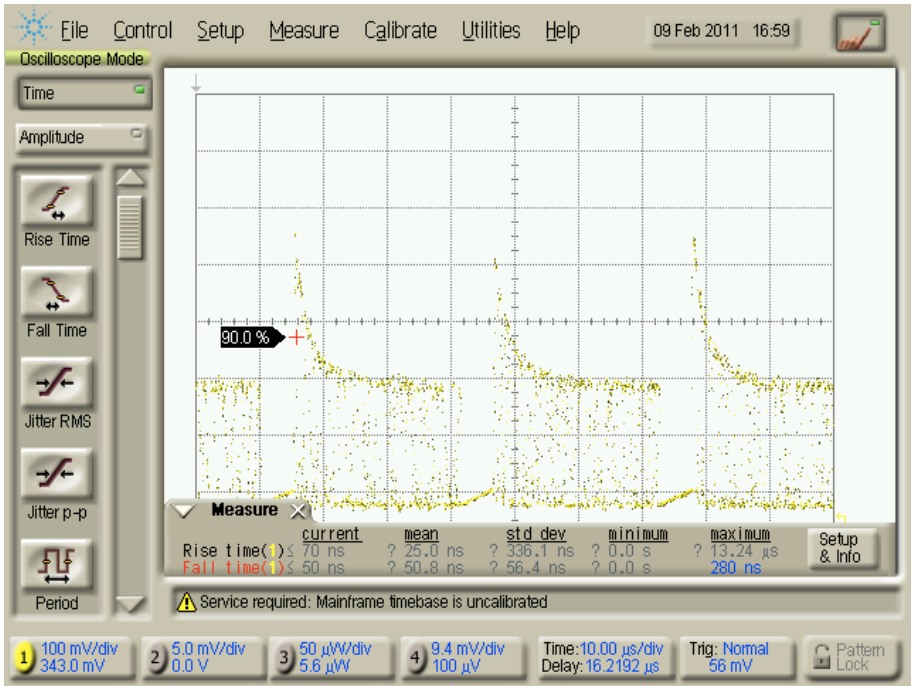

Figure 24: Example $2^{15\text{-}1}$ PRBS sequence amplified by an EDFA

As it can be deduced from the theory, trasient regime originates from the fact that the upper-state population is at its peak when the first incomning photons of a bursty packet start to be amplified and then quiclky and progressivly depletes, originating less amplfication.

If packets are small in bit number means that their photons can be amplifed before significant upper-state population is depleted, meaning that the transient regime will not be noticed for smaller packets.

Iddle times are important aswell, because during those iddle times the amplifier starts to re-populate its excited level. A satured EDFA amplifying non bursrty traffic will show no signs of transient beahaviour because its gain will stabilize at a value that translates a cyclical behavior of the dynamics between the fundamental and excited-state population: the excited state is depleted and re-populated at a constant rate and that results in a more stabilized amplification process.

This last paragraph is the basis of pump controlling and gain clamping schemes [24]. Those implementations intend to mimic the presence of non-bursty traffic by clampling the gain so its values are more stabilized and do not generate as much transience response, which is fundamentally expressed by the diference in gain between the first and last bits of packets.

The next stage of experimental procedures relates to preliminary transient acessements. This procedure consists in testing several sequences, iddle times, and pump power in order to determine where the transient regime is more notorious.

Firstly, a set of 20 sequences was prepared using the software included in the PRBS generator. Those sequences were divided in four groups, corresponding two four different packet lenghts: 2^5-1, 2^7-1, 2^{11}-1, 2^{14}-1. In each of those groups, five sequences with the corresponding packet length and a fixed number of zeros were assembled. The idle times corresponded to 1 μs, 25 μs, 50 μs, 75 μs and 100 μs.

Eight results from these measures where choosen to demonstrate the first two theorethical principles mencioned above. Figure 25 there shows 4 images taken from the digital osciloscope showing sequences of all studied lenghts and for the same idle time, 1µs.

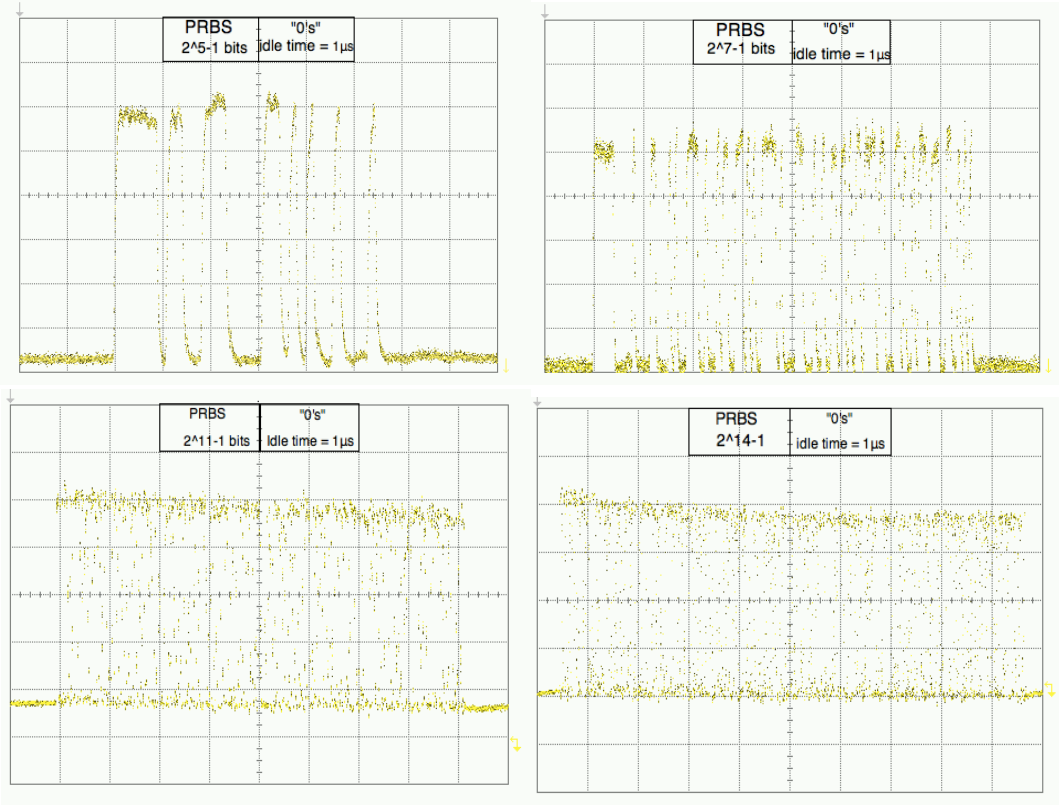

Figure 25: Temporal evolution of packets with the same idle time (1 µs) and differrent packet lenghts: 2^5-1, 2^7-1, 2^{11}-1 and 2^{14}-1 bits.

In the figure above only slight changes between the level of the first bits and remaining bits of the packet are noticed in the 2^{11}-1 and 2^{14}-1 length packets. Although, transient behavior is barely noticed since there is a very short period of time between packets and gain stabilization is quickly achieved.

If the idle time between packets is made longer, transient behavior is expected to be more notorious in the two longest packets but no changes are expected to happen in the two shortest packets, since the upper state population depletion for the amplification of such short number is not significant.

The idle time was risen to 25 µs and the results are shown in figure 26. As expected, transient behavior is exhibited strongly in the two last pictures that correspond to the two longer packets and no significant changes occur for the two shortest packages.

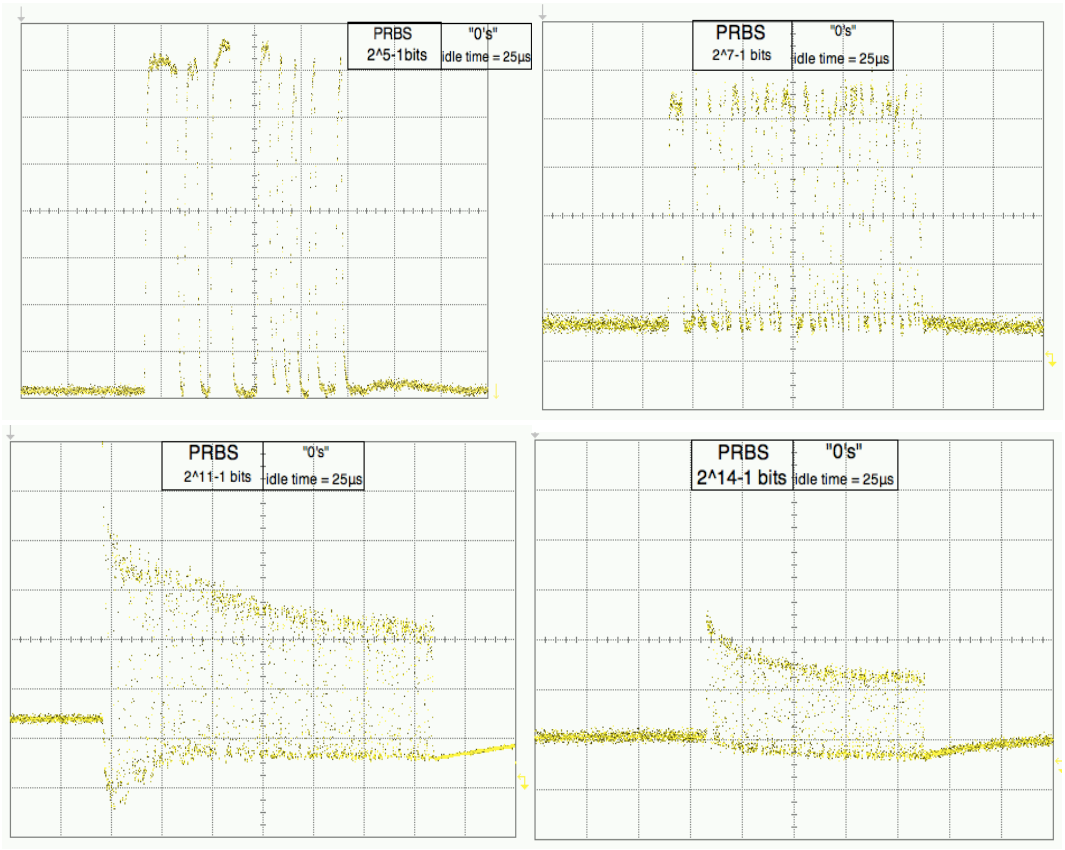

Figure 26: Temporal evolution of 4 packets with the same idle time (1 µs) and differrent packet lenghts: 2^5-1, 2^7-1, 2^{11}-1 and 2^{14}-1 bits.

In the characterization of the transience response phenomenon it is important to quantify packet distortion. The main trademark for packet distortion due to transience response is the exponential decay in power that packets seem to suffer when affected by transience, therefore the next experiments intended to go further in characterization. In order to do so exponential fittings were performed to all obtained data.

Pump power in the EDFA is an important parameter. It influences the amplification process and consequently transient response. The next experiment had a dual purpose: To study pump influence in packet distortion, since it is a relevant parameter, and to study the evolution of the decay term in an exponential fitting curve.

A PRBS sequence of 2^{14}-1 bits followed by 500 µs worth of zeros was used as test sequence. The data was taken from the same packet for several increasing currents in the EDFA pump laser (an increment in current is equivalent to an increment in pump power). Figure 27 shows the temporal evolution for the first value, 0.75A and for the last, 1.83A.

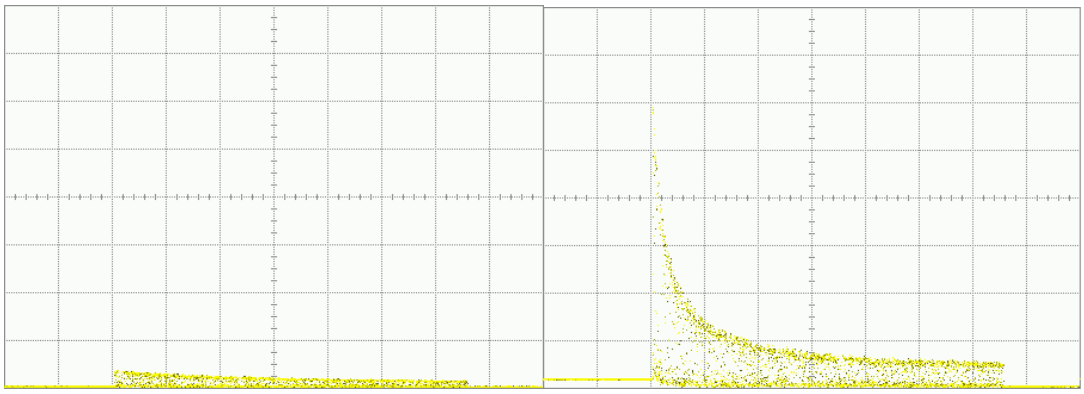

Figure 27: Temporal evolution of a PRBS 2^{14}-1 bit packet amplified by an EDFA with a pump current of 0.75A(left) and 1.83A(right).

Higher pump power represents higher excited state population and consequently more gain but it also represents a more accentuated decay in power as upper state population numbers quickly decrease.

In order to characterize in greater detail this decay exponential fittings where made to the packets

$$y = y_0 + A_1 e^{-(x-x_0)/t1}$$

The decay term of the equation, t1, increases as the curve approximates itself to a straight line, like in the case of lower pump currents. The practical meaning of this is that the more abrupt the changes in power, as in the case off higher pump currents, the smaller will be the values of t1. This is illustrated by plotting the function *exp(-x/t1)* for the values of the decay term shown in figure 28. An example of the data fitting for the signal amplitude envelope for a current of 1.83 A can be seen on figure 29.

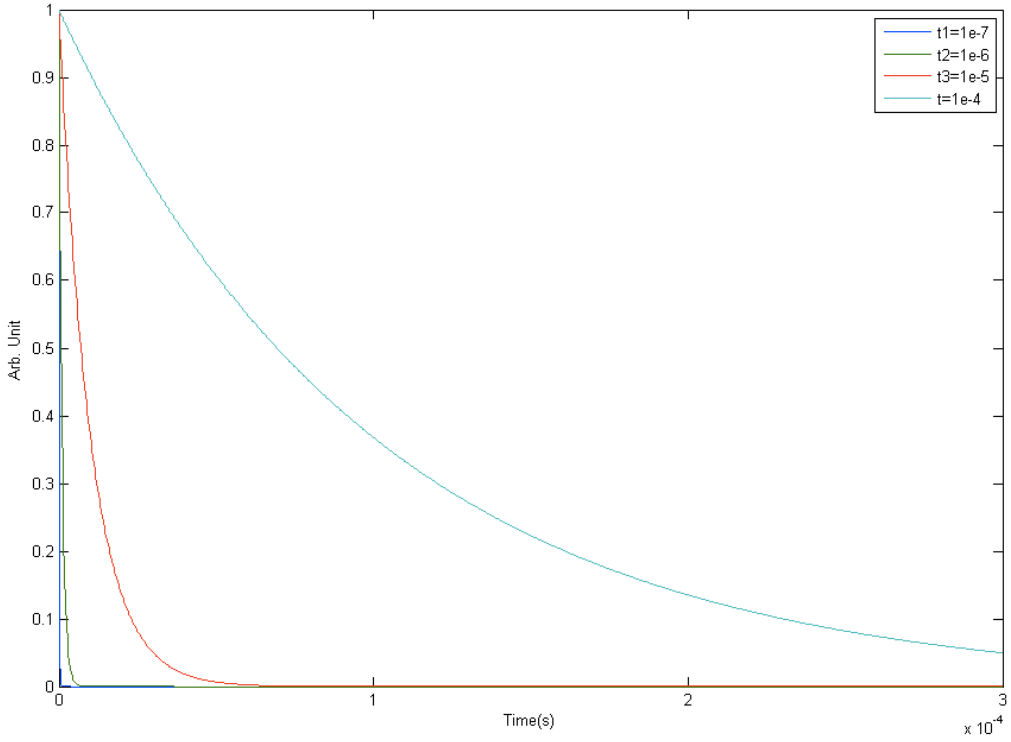

Figure 28: Example of packet distortion evolution with the values of the decay term.

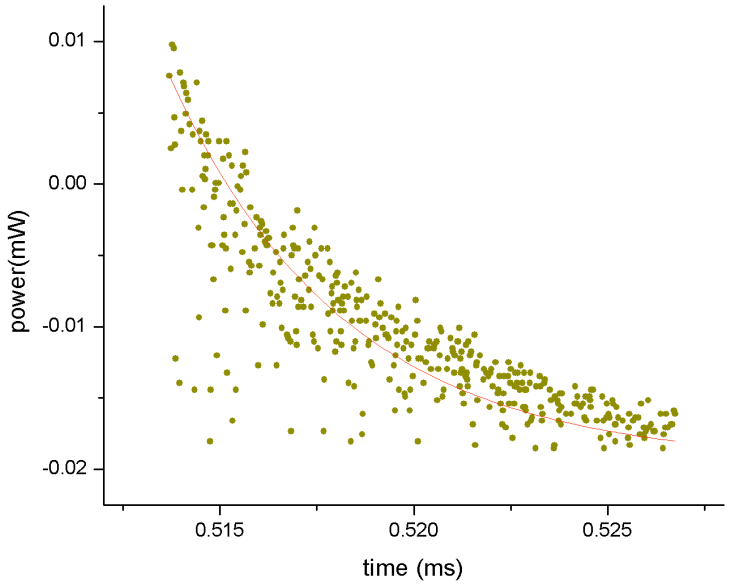

Figure 29: Experimental values the amplitude envelope of a data packet amplified by and EDFA with a current of 0.76 A.

The overall results can be seen on figure 30. The tendency is clear and it reveals extreme values when it comes to saturation currents as expected.

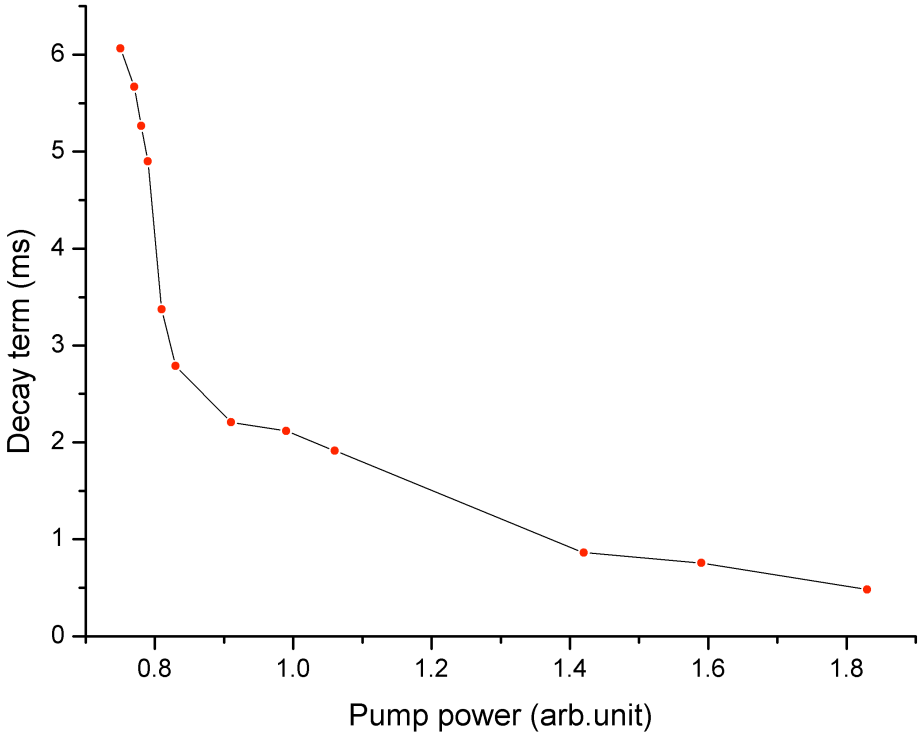

Figure 30: EDFA decay term, as a function of the pump power.

The next test relates to the practical validation of the numerical modeling of bursty traffic presented on chapter 3.

In order to test the effectiveness of the model, simulated packets were compared to experimental packets.

In order to determine how similar the results were, the exponential decay of packets for different idle times was calculated for both the experimental and simulation environments. The signal is composed by a fixed 2^{15}-1 PRBS sequence with duration of 26 μs followed by a variable idle time.

For the numerical simulation, an initial sequence of zeros with idle time 300 μs was conceived, being the only active channel the pump. This is done in order to the amplifier achieve full population inversion before packet amplification starts. After the initial sequence of 300 μs with no signal, two 2^{15}-1 PRBS sequences with a duration of 26 μs and separated by an idle time identically to the used in the experimental implementation was considered.

The typical values for the physical parameters of a saturated Erbium doped fiber were used, and choose an estimated pump power for a saturated EDFA of 0.3 W and signal power of 1 mW [23].

Figure 31 shows the experimental and simulated power evolution within the packet, for an idle time of 125 μs.

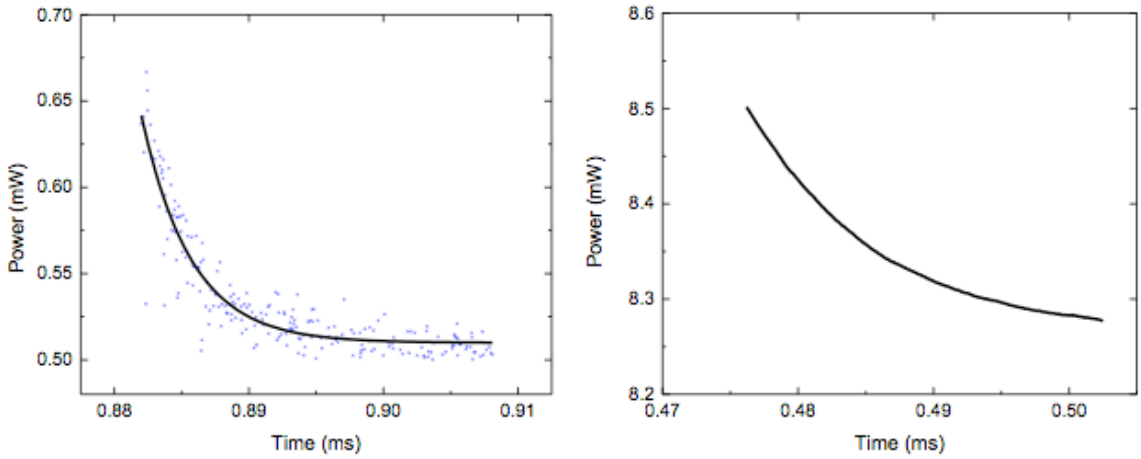

Figure 31: Experimental (left) and simulated (right) power evolution within the packet, for an idle time of 125 μs. On the left figure, points are experimental data and line is the fitting.

In figure 32 the results are summarized. The obtained decays the same order of magnitude is a promising result, since there is no full knowledge of the intrinsic parameters of the amplifier used in the experimental apparatus. These results show that this simplified model can potentially be used in the designing of EDFAs optimized for the minimization of the transients due to the bursty traffic.

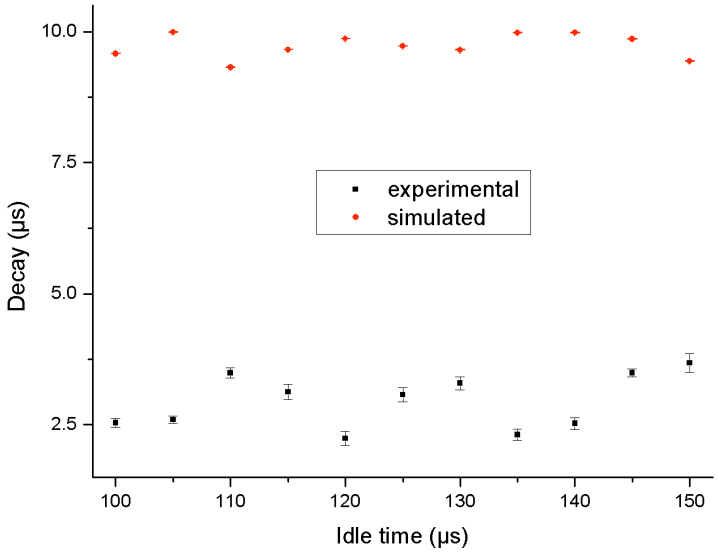

Figure 32: Obtained experimental and simulated decays terms for all tested idle times.

The decay term is not the only way to characterize packet distortion. The Q factor is often used to measure the packet quality [18].

The Q factor is given by the following expression:

$$Q = \frac{\mu_1 - \mu_0}{\sigma_1 + \sigma_0} \tag{4.1}$$

Where μ_1 is considered to be the medium value of the 1's level and σ_1 is considered to be equal to the amplitude of the same level. μ_0 and σ_0 are small variance terms that are negligible for this case.

μ_1 is obtained by isolating the 1's level with Matlab® and averaging all points. σ_1 is the difference between the maximum and minimum values of the acquired data set.

The raw data is supplied by the digital oscilloscope has negative power values that affect the calculation of μ_1. This is due to the fact that the oscilloscope converts optical power to an electrical voltage. In order to take out the negative values a power offset is added to every packet so that every value is positive.

The best scenario to test Q factor degradation is to do pump power study similar to the one illustrated in figure 31: the temporal evolution of 30 2^{14}-1 PRBS packets of increasing pump power separated by an idle time of 500 µs was measured and the Q factor was calculated using Matlab®. The obtained values were normalized, meaning that the best Q factor is equal to 1 and is associated with the lowest pump power used.

It is relevant to notice that these values translate precisely what's happening physically to the packets, which is a very high increase in maximum power values, which are the first bits of the packets to be amplified. As there is more population available for amplifying these first bits, their power will rise at a higher rate throughout the several measurements than the rest of the points considered. This is what originates the degradation of the Q factor with pump power ascension. A lower Q factor corresponds to a higher bit error rate (BER), which means that the receiver will have a harder task distinguishing which incoming signals are 0's or 1's. This is why transient regime seriously jeopardizes network performance. The summarized results in graphic form can be seen in figure 33.

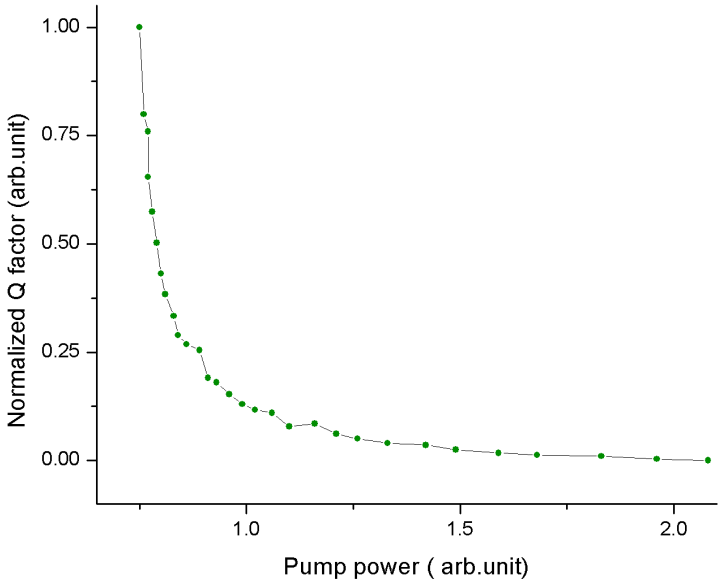

Figure 33: Normalized Q factor as a function of pump power

This concludes the experimental assessment. It was proved that both the decay term and Q factor are valuable parameters when it comes to transient regime characterization of EDFAs.

Packet size, pump power and idle time were proven to be fundamental variables in transient dynamics, as they affect directly the EDFA upper state population dynamics.

Chapter 5 - Conclusions and Future Work

In a different approach using graphical user interfaces, an EDFA steady state model was developed. The result was a fast and easy to use software tool that could be employed for multiple purposes. It is a tool that can be used in classrooms by students who are first learning about EDFAs, by undecided buyers and engineers who are not familiarized with models and want to make quick assessments.

Following the trend of making graphical user interfaces, an add/drop simulator up to 8 channels and 4 operations was built using a dynamic model based on the Saleh equations. The created Interface for the add/drop model serves the purpose of being a showcase model for future and more complex applications, programmed in a more suitable programming language, capable of handling dynamic changes in the interface's aspect with more easiness and less hardware processing time.

The dynamic model was explored further to simulate add/drop scenarios of limitless amounts of channels and see how transients arise from these particular operations.

Add/drop simulations play a key role in the investigation and industrial segments since large amounts of equipment are involved in these scenarios. Having software capable of simulating a high number of channels and predict the networks response to add and drop operations is a vital asset to any company or I&D institution has it is the most cost-effective way to study and prevent problems due to network reconfiguration and associated phenomena.

In an innovative way, the model was used to study the impact of bursty traffic in the EDFAs dynamic. The model uses the Runge-Kutta method, and its long computation times leave room for some relative improvement. These improvements where tried unsuccessfully by employing variations of the Runge-Kutta method, but the results where not consistent.

However, the model was validated successfully by comparing experimental packet power decays with their simulated counterpart. Results of the same order of magnitude where promising, since there was no full knowledge of the intrinsic parameters of the amplifier used in the experiment.

In the remaining experimental work, important conclusions about transient dynamic where withdrawn, such as the influence of pump current, the transient behavior on saturated EDFAs and the influence of packet length and idle time duration. It was shown that packets have to have enough length so that the transient effect is noted and that they need to be separated enough time so that the upper state population can be repopulated.

It was also demonstrated that pump current is a vital parameter, as it influences directly the packet excursion. The transient effect is particularly noticeable when the pump current is high and the EDFA is operating in a deep saturation regime.

It was stated and proved that both the packets decay term and Q factor are valuable parameters to calculate and analyze in order to successfully characterize the transient regime of EDFAs.

These are important contributions that can lead to the construction of more effective pump-controlled EDFAs and the design of intelligent passive optical networks that can reconfigure automatically in order to avoid the perturbations caused by EDFA's transient regime.

References

[1] Desurvire, E; "Capacity Demand and Technology Challenges for Lightwave Systems in the Next Two Decades," *Lightwave Technology, Journal of*, vol.24, no.12, pp.4697-4710, Dec. 2006

[2] Desurvire, E; , "Optical Communications in 2025," in *II Workshop Ciência e TecnologiaemComunicaçõesópticas*, Campinas, Brazil, 2005

[3] Hirosaki, B.; Emura, K.; Hayano, S.; Tsutsumi, H.; , "Next-generation optical networks as a value creation platform," *Communications Magazine, IEEE* , vol.41, no.9, pp. 65- 71, Sept. 2003

[4] Saaid, N.M.; , "Nonlinear optical effects suppression methods in WDM systems with EDFAs: A review," *Computer and Communication Engineering (ICCCE), 2010 International Conference on* , vol., no., pp.1-4, 11-12 May 2010

[5] Kani, J.-i.; , "Enabling Technologies for Future Scalable and Flexible WDM-PON and WDM/TDM-PON Systems," *Selected Topics in Quantum Electronics, IEEE Journal of* , vol.16, no.5, pp.1290-1297, Sept.-Oct. 2010

[6] R. J. Mears, L. Reekie, I. M. Jauncy, and D. N. Payne, "High gain rare-earth doped fibre amplifier at 1.54 pm," in Proc. Op- ticalFibreCommun. (OFC 87) (Reno, NV), 1987, paper W12.

[7] M. Wasfi, "Optical Fiber Amplifiers-Review," *International Journal of Communication Networks and* Information *Security (IJCNIS),* vol. 1, pp. 42-47, 2009.

[8] Xiang Zhou; Birk, M.; , "Performance comparison of an 80-km-per-span EDFA system and a 160-km hut-skipped all-Raman system over standard single-mode fiber," *Lightwave Technology, Journal of* , vol.24, no.3, pp.1218-1225, March 2006

[9] S. P. Singh. G. Ramgopal, "Gain optimization of an erbium-doped fiber amplifier and two-stage gain-flattened EDFA with 45nm flat bandwidth in the L-band," *Optik - International Journal for Light and Electron Optics,* pp. 77-79, 2010.

[10] Seoyong Shin; Daehoon Kim; Sungchul Kim; Sanghun Lee; SunghoSongtt; , "A Novel Technique to Minimize Gain-Transient Time of WDM signals in EDFA," *Optoelectronic and Microelectronic Materials and Devices, 2006 Conference on* , vol., no., pp.249-252, 6-8 Dec. 2006

[11]Reis, C.; Neto, B.; Dionisio, R.; Incerti, G.; Tosi-Beleffi, G.; Forin, D.; Rocha, A.M.;Teixeira, A.L.J.; Andre, P.S.; , "Transience analysis of bursty traffic with erbium Doped Fiber Amplifiers," *Transparent Optical Networks, 2009. ICTON '09. 11th International Conference on* , vol., no., pp.1-3, June 28 2009-July 2 2009

[12] T. G. Hogkinson, "Average power analysis technique for erbium-doped fiber amplifiers," *Photonics Technology Letters, IEEE,* vol. 3, pp. 1082-1084, 1991

[13] Naji, A.W.;Akhter, F.; Ibrahimy, M.I.; Ahmed, B.; Mahdi, M.A.; Siddiquei, H.R.; , "A computer based simulator for Erbium-Doped Fiber Amplifier," *Computer and Communication*

Engineering (ICCCE), 2010 International Conference on , vol., no., pp.1-5, 11-12 May 2010

[14] J. Girão, "Extender Box para Redes Ópticas Passivas GPON," MSc thesis, Departamento de Eléctrónica e Telecomunicações, University of Aveiro, 2010

[15] T. Almeida, "Dye-Doped OIH's for ligth amplification in Plastic Optical Fiber Systems," BSc thesis, Departamento de Física, University of Aveiro, 2008.

[16] A. A. Rieznik, "Modelagem e Física de Amplificadores a Fibra Dopada com Érbio," Msc thesis, Instituto de FísicaGlebWataghin, Universidade Estadual de Campinas, 2003.

[17] B. Neto, "Técnicas alternativas para amplificação de Raman em telecomunicações, "Ph.D thesis, Department of Physics, Universidade de Aveiro, 2010.

[18] M.Lima, A.Teixeira, "Apontamentos da disciplina de Comunicações Ópticas", Departamento de Electrónica e Telecomunicações da Universidade de Aveiro, Aveiro, 2010

[19] Bononi, A.; Rusch, L.A.; , "Doped-fiber amplifier dynamics: a system perspective," *Lightwave Technology, Journal of* , vol.16, no.5, pp.945-956, May 1998

[20] Awaji, Y.; Furukawa, H.; Puttnam, B.J.; Wada, N.; Chan, P.; Man, R.; , "Burst-mode optical amplifier," *Optical Fiber Communication (OFC), collocated National Fiber Optic Engineers Conference, 2010 Conference on (OFC/NFOEC)* , vol., no., pp.1-3, 21-25 March 2010

[21] C. R. Giles and E. Desurvire, ''Modeling erbium-doped fiber amplifiers,'' J. Lightwave Technol. 9, 271 – 283(1991).

[22] Saleh, A.A.M.; Jopson, R.M.; Evankow, J.D.; Aspell, J.; , "Modeling of gain in erbium-doped fiber amplifiers," *Photonics Technology Letters, IEEE* , vol.2, no.10, pp.714-717, Oct 1990

[23] A. Rieznik and H. Fragnito, "Analytical solution for the dynamic behavior of erbium-doped fiber amplifiers with constant population inversion along the fiber," J. Opt. Soc. Am. B 21, 1732-1739 (2004)

[24] Oliveira, J.C.R.F.; Rossi, S.M.; Silva, R.F.; Rosolem, J.B.; Bordonalli, A.C.; , "An EDFA hybrid gain control technique for extended input power and dynamic gain ranges with suppressed transients," *Microwave and Optoelectronics Conference, 2007. IMOC 2007. SBMO/IEEE MTT-S International* , vol., no., pp.683-687, Oct. 29 2007-Nov. 1 2007